

Modelling and Simulation of Heat Pump Systems for Hybrid and Electrical Vehicles

Mikael Eriksson and Oskar Graffman

Master of Science Thesis in Electrical Engineering
**Modelling and Simulation of Heat Pump Systems for Hybrid and Electrical
Vehicles**

Mikael Eriksson and Oskar Graffman
LiTH-ISY-EX--18/5152--SE

Supervisor: **Doktorand Olov Holmer**
ISY, Linköpings Universitet

Examiner: **Professor Lars Eriksson**
ISY, Linköpings Universitet

*Division of Automatic Control
Department of Electrical Engineering
Linköping University
SE-581 83 Linköping, Sweden*

Copyright © 2018 Mikael Eriksson and Oskar Graffman

Abstract

Hybridization and electrification of modern vehicles is today a reality. This effects the construction of the heating and cooling systems in vehicles where earlier the waste heat from the combustion engine was a great heat source. Heat pump systems are commonly used in heating systems in buildings and can therefore also be used for heating the cabin and different components in a vehicle. Modelling a heat pump system and performing simulations gives the advantage of investigating the heating performance of the heat pump during certain conditions. In this master thesis, which is performed in a pre-study project that is performed under the Swedish Electromobility Centre, a heat pump is modelled and the heating performance when changing the vapour quality is investigated during cold environments. Also how the heating capacity for different refrigerants and changing size and speed of compressor is simulated. With the methods and assumptions used, especially isentropic compression, the results shows that decreasing the vapour quality increase the mass flow in the heat pump circuit but the decrease in specific heating is larger which results in an overall decrease in heating capacity. The goal of 10 kW heating capacity can be achieved by increasing the compressor size or make use of waste heat from other vehicle components.

Acknowledgments

We would like to thank Scania and Martin Karlsson for giving us the opportunity to write this thesis. Specially we would like to thank our supervisor at Scania Ola Hall for all the help and for answering all our questions. Furthermore we would like to thank our supervisor at Linköping University Olov Holmer for helping us with simulation questions and and for great input on the report. Finally we would like to thank Professor Lars Eriksson for making this thesis a reality. The enthusiasm he shows when he is lecturing has increased our interest in the automotive industry.

Linköping, June 2018
Mikael Eriksson och Oskar Graffman

Contents

Notation	ix
1 Introduction	1
1.1 Motivation	1
1.2 Objective	2
1.3 Problem definition	2
1.4 Delimitations	2
1.5 Outline	3
2 Theory	5
2.1 First law of thermodynamics	5
2.2 Second law of thermodynamics	5
2.3 Heat transfer	6
2.3.1 Conduction	6
2.3.2 Convection	6
2.3.3 Radiation	6
2.4 Heat pump basics	7
2.4.1 Thermodynamic cycle	8
2.4.2 Compressors	9
2.4.3 Heat exchangers	10
2.4.4 Expansion device	19
2.5 Air Conditioner	19
2.6 Refrigerant	19
2.6.1 R134a	19
2.6.2 R1234yf	20
2.6.3 R744	20
2.7 Modelling	20
3 Related research	23
3.1 Heat pumps in vehicles	23
3.2 Waste heat recovery systems	25
3.3 Modelling and simulation of heat pumps	25
3.4 Two phase flow	30

4	Models	31
4.1	System overview	31
4.2	Working medium	32
4.3	Compressor	34
4.4	Condenser	35
4.5	Evaporator	40
4.5.1	Chiller	42
4.6	Expansion Valve	43
4.7	Simulink model	44
5	Results	47
5.1	Map function results	47
5.2	Modelling and simulation results	48
5.2.1	R134a	48
5.2.2	R1234yf	58
5.2.3	Step results	59
5.3	Validation results	59
6	Discussion	63
6.1	Method	63
6.2	Results	64
7	Conclusions	67
7.1	Conclusions	67
7.2	Further work	67
A	Appendix A	71
A.1	Map function plots	71
	Bibliography	75

Notation

ABBREVIATIONS

Abbreviation	Meaning
AC	Air Condition
BSFC	Brake Specific Fuel Consumption
COP	Coefficient of performance
EV	Electric vehicle
GWP	Global Warming Potential
HP	Heat Pump
LMTD	Logarithmic mean temperature difference
MPC	Model predictive controller
MTD	Mean temperature difference
MPPT	Maximum power point tracking
ODP	Ozone Depletion Potential
PID	Proportional-integral-derivative controller
TE	Termoelectric
TEG	Thermoelectric generator
TXV	Thermostatic expansion valve

NOMENCLATURE

Nomenclature	Meaning
A	Area
b	number of tubes/plates
C	Flow coefficient
c	Specific heat
d	Diameter
dz	Length element
E	Energy
f	Function
H	Enthalpy
h	Specific enthalpy
K	Mass flow times specific heat capacity
k	Conductivity
L	Length
m	Mass
N	Speed
Nu	Nussel number
n	Polytropic constant
\dot{m}	Mass flow rate
p	Pressure
T	Temperature
t	Time
Q	Heat transfer
\dot{Q}	Heat transfer rate
Pr	Prandtl number
q	Specific heat transfer
R	Gas constant
Re	Reynolds number
r	Thermal resistance
S	Entropy
U	Overall heat transfer coefficient
u	Specific energy
V	Volume
v	Velocity
W	Work
\dot{W}	Power/Rate of work
w	Specific work
x	Fraction of vapour
y	Thickness

NOMENCLATURE

Nomenclature	Meaning
α	Heat transfer coefficient
γ	Polytropic constant for isentropic process
ϵ	Emission constant
η	Efficiency
ρ	Density
σ	Stefan-Boltzmanns constant
ϑ	Specific volume
μ	Dynamic viscosity
Ψ	Watt per Kelvin

SUBSCRIPTS

Subscripts	Meaning
a	Air
c	Cross sectional
ci	Cold side inlet
ce	Cold side exit/outlet
CF	Counterflow
COOL	Cooling
comp	Compressor
cond	Condenser
evap	Evaporator
EXV	Expansion valve
h	Hot side
hi	Hot side inlet
he	Hot side exit/outlet
HP	Heat pump
i	Iterative number
in	Input
L	Liquid
LMTD	Logarithmic mean temperature difference
m	Mean
map	Mapping
max	Maximum
min	Minimum
MTD	Mean temperature difference
out	Output
p	Constant pressure
pol	Polytropic
r	Refrigerant
rad	Radiator
s	Surface
sat	Saturated
suc	Suction
tot	Total
V	Vapour
v	Constant volume
vol	Volumetric
w	Water
wg	Water/glycol
'	End of first zone
"	End of second zone

1

Introduction

1.1 Motivation

Hybridization of vehicles is a current topic in the automotive industry. Higher demands on more efficient vehicles, higher grade of hybridization and the using of more renewable energy sources for propulsion of the vehicles also lead to development of new techniques regarding heating systems. Today the heating of the cabin in vehicles is done by using waste heat from the combustion engine. There is a need of a heating system that can replace the lost heating capacity from the combustion engine waste heat when using the electrical drive in the hybrid system or purely electrical systems.

Heat pumps are used for transferring heat energy from a reservoir to a smaller restricted area, and is a common way of heating buildings. This technique can make use of the energy in a cold environment to heat a restricted area. The HP-system (heat pump) has the same components as an AC-system (air condition) that is a common cooling system used in most vehicles. This gives the possibilities of designing a heating system with already existing components. Using the HP technique for heat transfer in hybrid vehicles will contribute to a larger scale of hybridization and a longer range for renewable energy sources.

There is a need of a simulation model that can simulate the performance during special conditions, such as colder surrounding environments. The advantage of having a simulation model is that an investigation if the heat pump can deliver enough heat energy to heat the cabin can be made. Normally empirical models based on tests are made, but with a simulation model different configurations of the heat pump can be simulated, such as size of the heat pump and surrounding climate. Today a vehicle can be made in different shapes and sizes, and therefore there are different demands on how much heat capacity needed to heat the cabin and maintain a certain temperature on other components. A simulation model is

therefore an advantage compared to making test for the different configurations and different vehicle models.

1.2 Objective

The objective of the project is to learn more about and develop a heat pump system model. The project will contribute with knowledge of how to develop models and simulate a heat pump system in electrified vehicles, which in the future might be essential to further decrease the energy consumption. The project will also give knowledge of heat pump performance with varying vapour quality into the compressor. The heat pump model should be able to be integrated in an existing vehicle simulation platform.

1.3 Problem definition

Heat pumps are widely used for heating buildings and is a technique that has been well known for a long time. Integrating a heat pump in a vehicle has nowadays become an issue that is more discussed. This depends on the higher demands on vehicles with lower emissions, which leads to a higher demand on more renewable energy sources and new techniques. The main idea of integrating a heat pump into a hybrid vehicle is to heat/cool components and the cabin, and store energy from waste heat sources by making use of the thermal energy in a colder environment. The HP system is similar to the AC system that already exist in all modern vehicles. An AC/HP system that both cools and heats necessary vehicle components and the cabin is a future development.

An HP-system have certain dimensions and can operate with different refrigerants. Also the refrigerant can operate with different mass flow rates. This creates a design problem where the optimal dimensions, refrigerant and mass flow rate are interesting design parameters in the HP-system in a hybrid vehicle. The HP-system and AC-system has the same components, but the HP often need a larger volume flow to meet the heating demands in colder environments, which in this thesis is set to 10 kW. The mass flow rate can be increased by having a mixed phase of liquid and vapor. This thesis will explore the possibility to increase the heating capacity using this method. The compressor has a limitation of the composition of the mixture and this contributes to the design problem of the heat pump.

1.4 Delimitations

In this project the heat pump is only going to be used for heating and not for cooling. In case of model validation only data from AC tests are at disposal.

1.5 Outline

A short description of the content of the master thesis is described here.

Chapter 1, Introduction

This chapter includes the motivation, objective, problem definition and delimitations.

Chapter 2, Theory

This chapter includes the theory regarding heat transfer, heat pump components, air conditioner, refrigerants and modelling approaches.

Chapter 3, Related research

This chapter includes the related research regarding heat pumps in vehicles, waste heat recovery systems, modelling of heat pumps and modelling of two phase flow.

Chapter 4, Models

This chapter includes all the models of each component of the heat pump and the assembly of the whole model.

Chapter 5, Results

This chapter includes all the simulation results and the validation.

Chapter 6, Discussion

This chapter includes the discussion of the method and the results.

Chapter 7, Conclusions

This chapter includes the conclusions and possible future work.

2

Theory

2.1 First law of thermodynamics

The first law of thermodynamics is founded in that energy can not be lost, only be committed or transmitted into other energy forms. The equation for the first law of thermodynamics contains the heat transfer rate \dot{Q} , the rate of work \dot{W} , the temperature T , and the rate of mass \dot{m} . [8] The first law of thermodynamics for an closed system is expressed as:

$$mc_v \frac{dT}{dt} = (\dot{Q}_{in} - \dot{Q}_{out}) + (\dot{W}_{in} - \dot{W}_{out}) \quad (2.1)$$

where c_v is the specific heat capacity during constant volume.

The first law of thermodynamics for an open system with stationary flow can be expressed as:

$$\dot{m}c_p(T_{out} - T_{in}) = (\dot{Q}_{in} - \dot{Q}_{out}) + (\dot{W}_{in} - \dot{W}_{out}) \quad (2.2)$$

where c_p is the specific heat capacity during constant pressure.

2.2 Second law of thermodynamics

The second law of thermodynamics are based on the concept of entropy. The law treats the phenomena regarding the direction of the process. Heat can only during steady state transfer heat from a warmer source to a colder one. If the process can be reversed the entropy remains constant. If the process is irreversible the final entropy must be greater than the initial entropy. [8] The expression for the change of entropy is stated as:

$$\Delta S = \frac{\Delta Q}{T} \quad (2.3)$$

where ΔQ is the change of heat and T is the temperature.

2.3 Heat transfer

Heat transfer means that physical systems exchange thermal heat between each other. Heat transfer presents as conduction, convection and radiation.

2.3.1 Conduction

Heat transfer in form of conduction presents in fluids, gases and solids from molecules with a higher energy level to molecules with lower energy level. Conduction is defined as energy transfer from high energy regions to low energy regions. The heat rate can be defined as[8]:

$$\dot{Q}_{cond} = kA \frac{dT}{dy} \quad (2.4)$$

Where k is the heat conductivity, A is the area and $\frac{dT}{dy}$ is the temperature change with respect to the thickness of the material dy .

2.3.2 Convection

Convection is defined as heat transfer between a fluid in motion and a surface. There are two types of convection, forced convection and natural convection. Forced convection means that the flow is induced by a flowing device and therefore convection is created, and natural convection is not created by an flowing device. The heat rate in form of convection is defined as[8]:

$$\dot{Q}_{conv} = \alpha A_s \Delta T \quad (2.5)$$

Where α is the heat transfer coefficient, A is the surface area and ΔT is the temperature difference.

2.3.3 Radiation

The last form of heat transfer is radiation. Thermal radiation is emitted by all fluids, solids and gases. The calculation of thermal radiation is made by Stefan Boltzmanns law[8]:

$$\dot{Q} = \epsilon \sigma A (T^4 - T_0^4) \quad (2.6)$$

Where T is the body temperature, T_0 is the surrounding temperature, ϵ is the emission constant, A is the body area and σ is the Stefan-Boltzmanns constant.

2.4 Heat pump basics

A heat pump is used to transfer heat from one place to another, from a heat source to a heat sink. An example is the classic heat pump used to heat up either water or the indoor air in a house during the winter. A heat pump has the potential to work both as a heater (HP-mode) during winter and a cooler (AC-mode) during summer. The major components of a standard heat pump are expansion valves, a compressor, an indoor coil and an outdoor coil. The different coils work as an evaporator or a condenser depending on it being in HP-mode or AC-mode. Reversing valves are also required for switching between HP-mode and AC-mode. To understand this report a basic understanding of how a heat pump works is needed, so the following chapter will go into just that.

An air source heat pump, which is the heat pump used in this report, uses surrounding air to evaporate the refrigerant inside the evaporator. This is possible since the refrigerant has a lower boiling point than most common liquids (more on that in section 2.6). A fan is usually used to speed up this process. The low-pressure saturated vapor then enters the compressor, turning it into a high-pressure superheated vapor. The main purpose of the compressor is to move the refrigerant through the system and it is also here the input power of the system is, in form of electrical power. The high-pressure superheated vapor then enters the condenser, where another fan is used to blow air through the coil. Since the refrigerant is a lot warmer than the air a heat exchange between the two mediums will occur resulting in the refrigerant condensing into a high-pressure liquid. The heated air is then funneled to the desired heat sink. The refrigerant flows through the expansion valve where the flow is regulated leading to a pressure drop. This decrease in pressure is needed for the refrigerant to evaporate inside the evaporator. The cycle completes when the refrigerant once again enters the evaporator. This cycle is repeated again and again. [14]

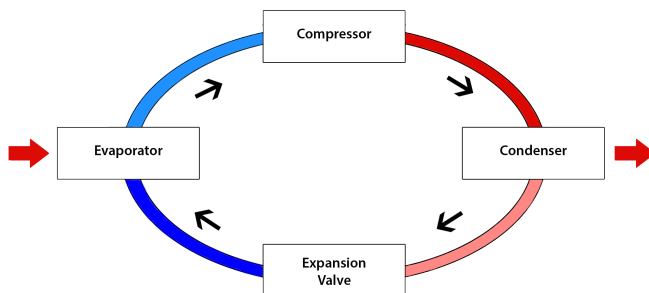


Figure 2.1: Image showing the working principle of a heat pump.

2.4.1 Thermodynamic cycle

The theoretical behaviour of the heat pump can be described by the temperature-entropy plot and the pressure-enthalpy plot. [33]

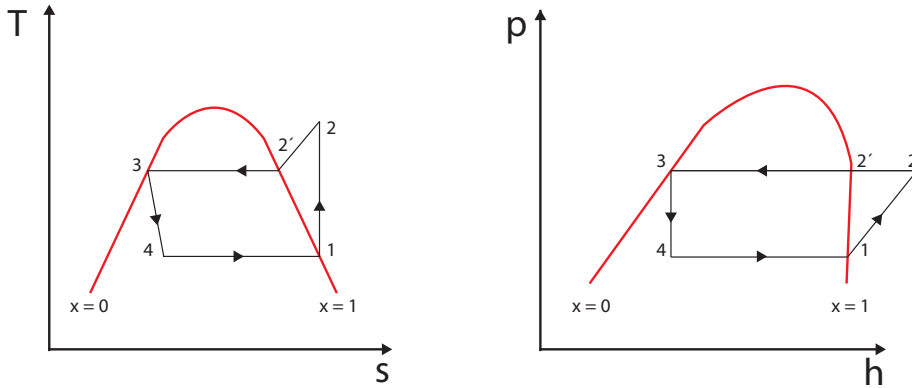


Figure 2.2: Figure showing the t - s diagram and the p - h diagram. The red lines are the saturation limit and x stands for the fraction of vapor in the mixed phase region.

Figure 2.2 shows all the thermodynamic stages in the theoretical heat pump. Between (1-2) in the image there is a isentropic compression which raises the pressure and temperature. Isentropic compression means that there is no heat exchange with the surroundings and the process is reversible. As seen the entropy in the left image will not change during the isentropic compression. This stage represents the part when overheating saturated vapor in the compressor.

The next stage between (2-2') is an isobar process where the overheated vapor becomes saturated vapor. The stage between (2'-3) is an isobar and isotherm process where saturated vapor becomes saturated liquid. This theoretical stage represents the condenser part in the heat pump.

The stage between (3-4) is where the refrigerant enters the expansion valve and goes from saturated liquid to a mixed phase. This process is an isenthalpic lamination where both the pressure and temperature is decreased.

Then the last stage between (4-1) is represented by the evaporator in the heat pump. This is a isobar and isotherm process where the mixed-phase goes to saturated vapor by absorbing heat from the environment.

The theoretical cycle has the following equation for added specific work during the compression:

$$w = h_2 - h_1 \quad (2.7)$$

Where h is the specific enthalpy. When the condenser releases heat to the environment the following equation explains the specific heating:

$$q_{cond} = h_2 - h_3 \quad (2.8)$$

In the evaporator the specific cooling can be expressed as:

$$q_{evap} = h_1 - h_4 \quad (2.9)$$

One of the most important parameter for a heat pump is the coefficient of performance (COP). COP essentially says how much energy output is produced for a specific energy input, same thing applies for input/output power.

The input power of the system is, as mentioned above, the compressor power. The power absorbed by the refrigerant is depending on losses such as pipe losses, shell losses of the compressor. Assuming that the compressor is adiabatic:

$$\dot{W}_{comp} = \dot{m}_r w = \dot{m}_r (h_2 - h_1) \quad (2.10)$$

where \dot{m}_r and h is the mass flow rate and the enthalpy of the refrigerant.

The output power for this system is heat absorbed by the fluid from the condenser, it can be calculated using the first law of thermodynamics:

$$\dot{Q}_{cond} = \dot{m}_r q_{cond} \quad (2.11)$$

The COP of the system is therefore calculated using:

$$COP = \frac{\dot{Q}_{cond}}{\dot{W}_{comp}} \quad (2.12)$$

2.4.2 Compressors

Positive displacement compressors and dynamic compressors are two classes of compressors. There are also sub classes of compressors which is shown in Figure 2.3. [33]

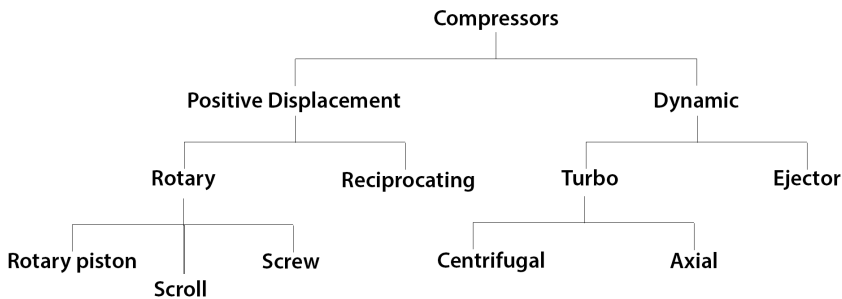


Figure 2.3: Figure showing different classes and subclasses of compressors.

These compressors are often semihermistic or hermistic, which means that the motor that is driving the compressors will be cooled by the refrigerant passing the compressor. The motor can also be placed outside the refrigerant system. [33]

Positive displacement compressors are also divided into the sub classes Reciprocating compressors and rotary compressors. In Reciprocating compressors a piston is used to compress, and in rotary compressors either a spiral, screws or pistons perform a rotary motion to compress. [33]

The most commonly used compressors for heat pump operations are positive displacement compressors and turbo compressors. The main abilities of these compressors are that there is a high compression ability by single state compression, there is no restriction on the suction pressure and when transporting the refrigerant there is lack of continuity. In the subclass Rotary compressors there is a rotational motion to compress the vapor. The rotary screw compressor has two meshing rotary screws that rotate in different directions and decrease the volume along the screws. A scroll compressor has two parts formed as spirals and is often used to compress air or refrigerant. The turbo compressor has the ability of factor reduced compression and increasing the flow of the refrigerant. What kind of compressor that should be used in a certain application depends on the thermal power, which refrigerant that is used and installation. [19]

2.4.3 Heat exchangers

A heat exchanger is a device that transfers thermal energy between two fluids, a solid material and a fluid or a fluid and a solid material. The typical applications that heat exchangers are used in are recovering heat, rejecting heat, condensing and evaporating.

Classification of heat exchangers

Heat exchangers are normally classified depending on transfer process, number of fluids, heat transfer mechanism, but are also classified by construction type, flow arrangement, heat transfer surface area/volume ratio, compact/non-compact. [28]

The heat exchanger transfer process can either be indirect or direct. If the heat exchanger is a direct transfer type it means that the heat is exchanged between two fluids separated by a wall and the fluids have separate flows. The heat transfer surface transfers heat between the fluids by conduction. If the heat exchanger on the other hand is of indirect transfer type it means that there is an intermittent heat exchange between the fluids.

Most processes where a heat exchanger is used two or more fluids are used, and therefore there is a classification based on the number of fluids. The most common configuration is a two fluid heat exchanger which is widely used, but multi flow exchangers are used in the chemical industry.

The classification regarding compactness is based on the heat transfer area per unit volume that is possible for the exchanger. The compactness is important when adapting to a limited space, reducing weight, energy requirements, costs, layout and design. The compactness of the exchanger is also dependant on the flow arrangement. For a two flow compact heat exchanger it is common to have counter flow, cross flow, or multi flow as flow arrangement.

Heat exchangers come in different shapes and constructions. The exchangers are most common classified as tubular, plate type, extended surface and regenerative exchangers.

The flow can in a heat exchanger be arranged in different ways, such as single pass and multi pass exchangers. In single pass exchangers the flow can be arranged as counter flow, parallel flow or cross flow.

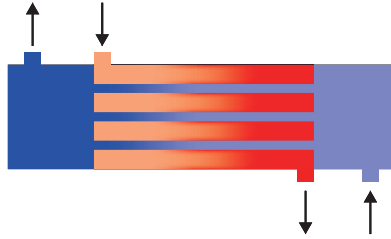


Figure 2.4: Figure showing the flow arrangement and temperature change in a counter flow heat exchanger.

In a counter flow exchanger two fluids flows in different directions relative to each other shown i figure 2.4. Counterflow is the most efficient flow arrangement compared to other two flow arrangements where the temperature change allows the exchanger to be treated as one dimensional [28].

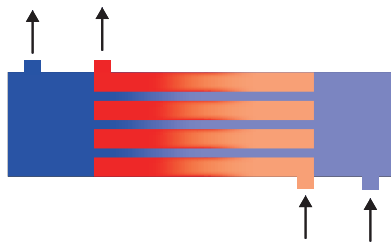


Figure 2.5: Figure showing the flow arrangement and temperature change in a parallel flow heat exchanger.

In parallel flow exchangers the flow of the two fluids flows in the same direction which is shown in figure 2.5. The parallel flow arrangement has the lowest efficiency compared to the other single pass exchangers [28].

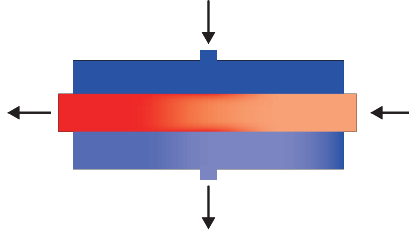


Figure 2.6: Figure showing the flow arrangement and temperature change in a cross flow heat exchanger.

The last type of flow arrangement is cross flow where the two fluids flow in a direction perpendicular to each other. The effectiveness of the cross flow exchanger falls between the two other earlier mentioned single pass flow arrangements. Depending on the design of the exchanger mixing between steam and fluid can occur. A multi pass exchanger has a number of single pass exchangers arranged in a certain series construction. This type of flow arrangement is implemented when having low flow velocities, low efficiency or extreme length.

In the last classification the heat exchangers are classified depending on the heat transfer mechanism. The heat transfer mechanism can be single phase on both sides of the exchanger, single phase on one side and two phase on the other, two phase on both sides, combined convection and radioactive heat transfer. [28]

The evaporator is a heat exchanger which main task is to exchange heat from the outside fluid/gas to the refrigerant. The refrigerant has a low pressure and temperature at the inlet to the evaporator. Entering the evaporator as wet vapor further on leads to exiting the evaporator as saturated vapor according to the ideal vapor-compression cycle shown in figure 2.2. The evaporator is formed as a coil and is often ordered in several rows. The heat exchange occurs when the air passes transversely to the tubes. The same structure is applied at the condenser but the heat exchange goes from the refrigerant to the fluid/gas. [11]

Energy and mass conservation equations

The heat exchanger can be treated as a control volume where mass and energy is stored. According to the first law of thermodynamics and by neglecting the kinetic and potential energy, the energy change in the heat exchanger can be expressed as:

$$\frac{dE_{cv}}{dt} + \frac{\partial \dot{m}h}{\partial t} = \dot{Q} \quad (2.13)$$

Where there is no work added to the control volume. The heat transfer \dot{Q} can be expressed with equation 2.5 for convection. The energy for the heat exchanger control volume can be expressed with the following equation:

$$E_{cv} = A_c \rho dz u = A_c \rho dz \left(h_{cv} - \frac{p}{\rho} \right) \quad (2.14)$$

Where u is the specific energy, A_c is the cross sectional area, p is the pressure, dz is the integrating length element, h_{cv} is the specific energy of the control volume. The specific enthalpy of the control volume can on the other hand be expressed with the following mean value equation:

$$h_{cv} = h_{in} + \frac{1}{2} \cdot \frac{\partial h}{\partial t} dz \quad (2.15)$$

The equations 2.5, 2.14 and 2.15 together with the assumption of neglecting second order terms gives the following energy balance for the heat exchanger:

$$A_c \frac{\partial(\rho h - p)}{\partial t} dz + A_c \frac{\rho v h}{\partial z} dz = \alpha A_s dz \Delta T \quad (2.16)$$

Where A_s is the surface area v is the velocity.

The conservation of mass in the control volume can be written as:

$$\frac{dm}{dt} = \dot{m}_{in} - \dot{m}_{out} \quad (2.17)$$

Vapour quality

During the evaporation and condensing process the fluid change phase and the three phases are liquid, mixture of liquid/vapour and vapour. There are two common concepts that describes the phase change in the mixture, which is quality and mean quality.

The quality of the mixture out from the heat exchanger is defined as the content of how much gas and how much liquid the mixture contains. The equation for the quality of the fluid can be written as:

$$x = \frac{h - h_L^{sat}}{h_V^{sat} - h_L^{sat}} \quad (2.18)$$

where h_L^{sat} and h_V^{sat} is the specific enthalpy for saturated liquid and vapour.

The mean vapour quality is defined how much mass of the total mass that is gas. The equation for the mean vapour quality for the mixture zone can according to Andersson and Jerregård [6] be written as:

$$x_{mean} = \frac{m_V}{m_V + m_L} \quad (2.19)$$

Where m_V is the mass of gas and m_L is the mass of liquid in the two phase region.

Overall heat transfer coefficient

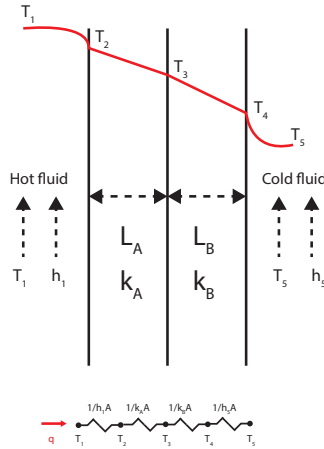


Figure 2.7: Figure showing configuration for calculating the overall heat transfer coefficient.

The overall heat transfer coefficient is defined by Newtons law of cooling as:

$$U = \frac{1}{r_{tot}A} \quad (2.20)$$

Where r_{tot} is defined as the sum of all thermal resistances which is shown in figure 2.7. The sum can be written as:

$$r_{tot} = \sum \frac{1}{r_i} \quad (2.21)$$

Temperature change in heat exchangers

The total rate of heat flow between the hot and cold side can in a heat exchanger in general be expressed with the following equations:

$$\dot{Q}_h = \dot{m}_h(h_{hi} - h_{he}) \quad (2.22)$$

$$\dot{Q}_c = \dot{m}_c(h_{ci} - h_{ce}) \quad (2.23)$$

This with the assumption that changes in the kinetic and potential energy is negligible and there is no heat transfer with the surroundings. If there is no phase change the temperature on the heat rate equations above can be rewritten with respect to the temperature.

$$\dot{Q}_h = \dot{m}_h c_{p,h}(T_{hi} - T_{he}) \quad (2.24)$$

$$\dot{Q}_c = \dot{m}_c c_{p,c} (T_{ci} - T_{ce}) \quad (2.25)$$

In these two equations the specific heat coefficients are assumed to be constant. The figure below shows how the temperature changes across a parallel flow heat exchanger.

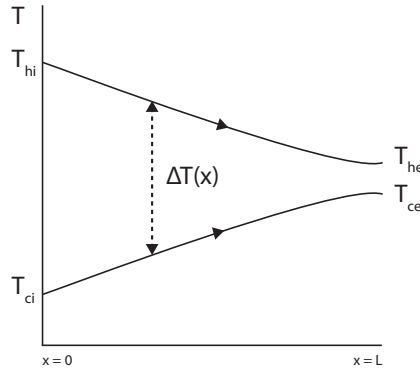


Figure 2.8: Figure showing the temperature change on the hot and cold side of the parallel flow heat exchanger.

The temperature on the hot and cold side will change with respect to the length of the heat exchanger. In a parallel flow heat exchanger the temperature on hot side will decrease and on the cold side increase in a way illustrated in figure 2.8. The temperature difference between hot and cold side will be large when $x = 0$ and decrease with the length of the heat exchanger. The figure below shows how the temperature changes across a counter flow heat exchanger.

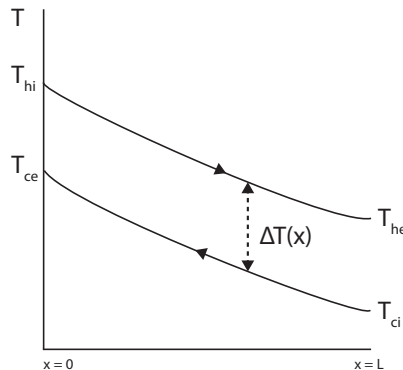


Figure 2.9: Figure showing the temperature change on the hot and cold side of the counter flow heat exchanger.

In a counter flow heat exchanger the temperature difference between the hot and cold side will change less with the length of the heat exchanger, which is

illustrated in figure 2.9. The temperature difference can be expressed with the following equation:

$$\Delta T(x) = T_h(x) - T_c(x) \quad (2.26)$$

The temperature difference varies with the length of the heat exchanger and therefore the heat transfer can be expressed as:

$$Q = UA\Delta T_m \quad (2.27)$$

Where U is the overall heat transfer coefficient, A is the area and ΔT_m is the mean temperature difference.

The mean temperature difference can be calculated in a several ways. One way is to take the average temperature difference between the hot and cold side.

$$\Delta T_{m,MTD} = \frac{1}{2}((T_{hi} + T_{he}) - (T_{ci} + T_{ce})) \quad (2.28)$$

Another way of calculating the mean temperature difference is written by P.Incropera et al. [32] and is called logarithmic mean temperature difference.

$$\Delta T_{m,LMTD} = \frac{\Delta T_1 - \Delta T_2}{\ln \frac{\Delta T_1}{\Delta T_2}} \quad (2.29)$$

Where ΔT_1 is the difference between hot and cold inlet temperature and ΔT_2 is the difference between hot and cold outlet temperature. The most important thing to consider when selecting the mean temperature difference equation is that the $T_{m,MTD}$ is overestimating the temperature difference.

When considering a cross flow heat exchanger the heat transfer can according to P.Incropera et al. [32] be calculated by the following equation:

$$Q = bkA_s\Delta T_m \quad (2.30)$$

Where b is the number of tubes, k is the conductivity and A_s is the surface area.

When the working medium in the heat exchanger is shifting phase the temperature does not change on the working medium as can be seen in figure 2.10 and 2.11.

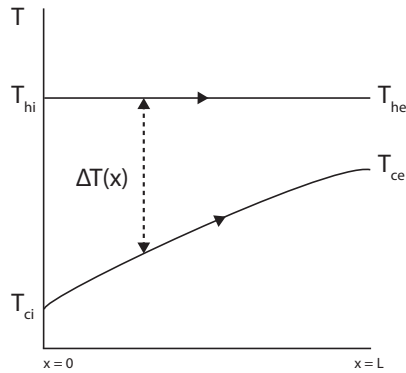


Figure 2.10: Figure showing the temperatures inside the condenser vary with the length of the parallel flow heat exchanger.

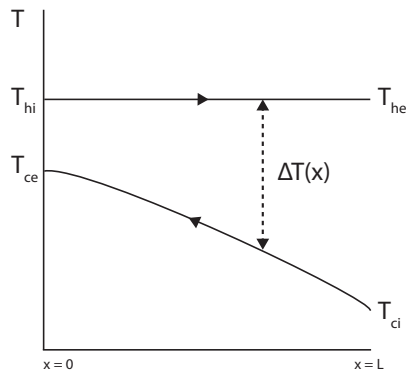


Figure 2.11: Figure showing the temperatures inside the condenser vary with the length of the counter flow heat exchanger.

How the condensing temperatures changes in the heat exchanger is shown in figure 2.10 and 2.11. During the condensing process the cold side of the heat exchanger increases in temperature with the length while the working medium has a constant temperature as.

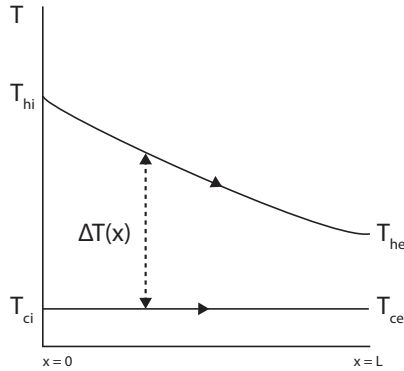


Figure 2.12: Figure showing the temperatures inside the evaporator vary with the length of the parallel flow heat exchanger.

During the evaporating process the hot side temperature decreases with the length of the exchanger while the working medium temperature stays constant, which is shown in figure 2.13.

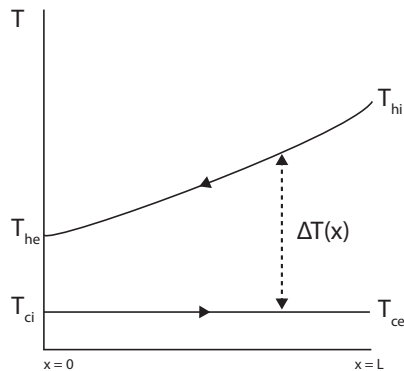


Figure 2.13: Figure showing temperatures inside the evaporator vary with the length of the counter flow heat exchanger.

Pinch point

A problem that has to be taken into consideration when modeling a heat exchanger is the pinch point which is the point where the temperature of the hot and cold fluid are the closest. The problem occurs since the heat exchanger cold side temperature cannot cross the hot side temperature since that would violate the second law of thermodynamics.

2.4.4 Expansion device

After the condenser the refrigerant needs to be expanded so that the temperature of the refrigerant is lower than the heat source in the evaporator. This is done by an expansion valve or some other kind of throttling device. The liquid out from the condenser will be accelerated to a higher flow through the expansion valve. An expansion device can be used to keep the superheated temperature at the evaporator outlet or the subcooling at the condenser outlet at a fixed value by controlling the pressure drop with the cross sectional area. The expansion device cooperates with the compressor to achieve the required pressure differences over the heat pump.[11]

2.5 Air Conditioner

As mentioned earlier, AC is the method used today for cooling the air inside the passenger compartment. Unlike the heat pump an air conditioner can only work as a cooling system and is incapable of heating the passenger compartment during winter conditions. Like the heat pump an AC-unit uses a **compressor** to increase the pressure of the refrigerant as well as pushing it through the system. The high pressure refrigerant then travels through the **condenser** where a fan blows cool ambient air on it. The ambient air cools the refrigerant making it condense. The refrigerant then goes through an **expansion valve**, lowering the pressure. The evaporator, which is placed near the dashboard of the vehicle, is the last component of the cycle. The warm air from inside the passenger compartment blows through the **evaporator** making the refrigerant evaporate and the warm air cools down to a more comfortable temperature. [4]

The AC-mode of the heat pump works in the exact same way.

2.6 Refrigerant

As mentioned above, a refrigerant is used for transferring heat inside the heat pump. The main reason for using a refrigerant is that the boiling point is usually lower than most common liquids, which means that the liquid can evaporate at lower temperatures. This boiling point can be controlled by altering the pressure on the refrigerant. Therefore the "pressure/temperature" relationship is one of the most important characteristics of the refrigerant. [20]

There are a lot of different refrigerants to choose between and some factors to take into consideration when choosing refrigerant are: cooling capacity, safety, environmental impact, ease of use, cost and the availability of components.

2.6.1 R134a

R134a, also known as HFC-134A is an extremely common refrigerant used for a wide variety of application. It belongs to hydrofluorocarbons (HFCs) and was developed to replace chlorofluorocarbon (CFC) which damages the ozone layer

[8]. Advantages for R134a are that it is safe for normal handling, non-toxic, non-corrosive, non-flammable and a zero ODP(Ozone Depletion Potential). A disadvantage is that it is classified as a greenhouse gas and contributes to global warming. R134a has a GWP(Global Warming Potential) of 1430 (medium) [2] while R744 has a GWP of 1 (low) [3].

2.6.2 R1234yf

R1234yf is a next generation refrigerant and is said to become the replacement of R134a. R1234yf is a non-toxic hydrofluoroolefin (HFO) with its biggest advantages being the low GWP of 4. [1] Similar to R134a the Ozone Depletion Potential is zero. The refrigerant is commonly used for refrigerators and mobile air conditioning. It is slightly flammable and is therefore not suitable for already existing R134a systems.

2.6.3 R744

R744 (CO_2) is one of the multiple refrigerants to choose from. It is an environmentally friendly refrigerant having zero ODP and minimal GWP. With its excellent thermodynamic properties and low energy usage R744 is suitable for many different applications. The biggest difference compared to other refrigerants is its high operating pressure and low critical temperature, meaning that the system require special equipment designs [3]. R744 as a refrigerant has demonstrated favorable results in several configurations over many years across the world. This combined with the environmental advantages leads people to believe R744 is a long-term option in the foreseeable future. [15]

When taking the factors mentioned above into consideration R744 offers a superior cooling capacity than other conventional refrigerants while having a significantly lower GWP. R744 has low toxicity (at low concentrations) and is non-flammable but the high operating pressure issues some challenges by requiring a more complex system. The cost of the refrigerant is fairly low while the system cost is higher than other conventional systems. The biggest potential hazards of using CO_2 as the refrigerant are the high pressure, toxicity at high concentration and the potential for dry ice formation. These hazards needs to be taken into consideration.

2.7 Modelling

A model of a system is a tool for answering questions about a system without experiments. Imagine one are unable to perform an experiment or it is too expensive, a model of that said system can calculate and determine how the system would behave. A mathematical model, which is a usually used model for technical systems, solves equations that describes the system.

There are two ways to create a mathematical model which describes a system. One way is to gather information and experience from experts and literature within the field. By using this method one gets a detailed model for the heat

exchangers which is based on fundamental heat and mass transfer relations. The other one is by observing the system itself. This is called system identification and uses observations of the system to find a suitable model. This type of model is also known as a **Black box** model since it only describes the relationship between input and output without caring about the underlying physical equations. These models are often simple and highly empirical.

These two extremes are often combined into what is known as a **Grey box** model where the model is constructed from basic physical principles and some parameters represent unknown values of the system. [29]

Table 2.1 shows a description of different types of models.

Table 2.1: Description of different types of models.[29]

Model Type	Time variation of system inputs/outputs	Model complexity	Physical understanding	Type of equation
Simulation model	Dynamic Quasi-static	White box Detailed mechanistic	High	PDEs ODEs
Performance model	Quasi-static Steady-state	Grey box Semi-empirical Lumped	Medium	ODEs Al-gebraic
Performance model	Static or Steady-state	Black box Empirical	Low	Algebraic

Mathematical models can be divided into different classes. **Deterministic** models only use exact relations between measurable and derived variables. A deterministic model is therefore without insecurities. A model is considered a **stochastic** model if it also uses insecurity or probability concepts.

A system is often characterized by several variables changing with time. Sometimes there are instantaneous relationships between those variables, these models are called **static**. Almost all models, even if the overall system is of dynamic nature, includes subsystems that are static.

For some system the variables change without external impact and therefore their values depend on previously calculated signals. These models are called **dynamic**. Dynamic models usually include differential equations.[29] These are only a few of all the classes which mathematical models are divided into.

3

Related research

3.1 Heat pumps in vehicles

In Hosoz and Direk [22] the usage of an integrated AC and HP system in automobiles with R134a as refrigerant is studied. By reversing the flow of the refrigerant in the AC circuit a HP circuit can be achieved and the system will heat the cabin instead of cooling the cabin. The study treats experiment of a AC/HP system. The experiment setup contains two fan arrangements, a compressor, a reversible valve for flow direction of the refrigerant, a electric heater and two coils acting as evaporator/condenser. Due to this setup in the first test the outdoor fan speed where fixed at a high speed which created a fixed air flow and further the compressor speed where increased and then at last the required indoor temperature could be reached by using a electric circuit. In the second test the condenser temperature where set to a fixed value and the fan speed where changed to create different air flow. During these tests the condenser temperature where set to a fixed value (45°C, 50°C, 55°C). The coil that is designed as a condenser also works fine as a evaporator, and vice versa. One interesting result is that the coil that originally works as a evaporator in AC mode can not work as a condenser adequately which means that when having a AC/HP system there is a need for a greater coil area and a greater refrigerant flow. The cooling and heating capacity is increasing and the COP value is decreasing with increased compressor speed. In HP mode the amount of heat transferred to the indoor coil is enough to use in automobiles in mild climate conditions, in other conditions the HP is considered as a compliment to other heating systems.

Jokar et al. [26] uses two separate secondary loops containing a 50 % glycol-water mixture in addition to a standard heat pump system. The purpose of the extra loops are to exchange energy with the refrigeration loop. The system used

had a heat pump (HP) mode and an air conditioning (AC) mode that can be used during winter and summer conditions. The system was set up so that both the ambient air and the cabin air are in contact with the secondary loops instead of the standard refrigeration loop, i.e. one secondary loop were between the heater core and the condenser while the other is placed between the external heat exchanger and the evaporator. The coefficient of performance for HP mode ranged between 2 and 5 depending on the conditions.

The biggest problem with these results is that the "winter conditions" studied in this article are fairly mild (9-10°C) compared to Nordic winter conditions (which is of interest in this report).

Hosoz et al. [23] evaluate both transient and steady-state performance parameters for a experimental heat pump system using R134a as refrigerant with three different heat sources. This was done by measuring the parameters after the first five minutes and also during steady state. The heat sources were ambient air, engine coolant and the exhaust gas, these were then compared to the baseline system. The system is coupled to the passenger compartment of a test vehicle. The parameters studied include: mean air temperature in the passenger compartment, air temperature at the compartment front register outlet, heating capacity, COP and the increase in brake specific fuel consumption (BSFC). The tests were operated at different engine/compressor speeds with a fixed air temperature at the inlets of the indoor and outdoor coil of 5°C.

Conclusions for idling conditions that can be drawn from these test are that a heat pump with any of the three heat sources gives a higher temperature and heating capacity compared to the baseline system after 5 min while the heat pump with engine coolant as a heat source provides the highest air temperature and heating capacity during steady state.

An interesting result is that with increasing engine torque and speed the baseline provides a higher heating capacity after steady state has been achieved. The heat pump with the engine coolant as a heat source is the only one with a higher heat capacity than the baseline for higher engine speeds ($N > 850$ rpm) The coefficient of performance is the highest for the system with the engine coolant and the lowest for the system with the ambient air.

Katayama et al. [27] developed a heat pump water heating system and compared it to a mass produced system equipped with an electric water heater. The tests were done while the engine was off with the goals of increasing the level of comfort and saving power. The conclusions drawn from the tests are that when utilizing a heat pump water heating system instead of a electric water heater the power consumption is reduced by 40% while maintaining the same level of comfort. By using a heat pump instead of a electric water heating system should increase the EV-driving (when the engine is turned off) mileage drastically. According to Katayama et al. [27] it might be possible to increase the efficiency and level of comfort even further by increasing the efficiency of the compressor and make it as small as possible.

Domitrovic et al. [13] simulated a model for steady-state operation with the goals of studying the effectiveness and performance of heat pumps for automotive use. The heat pump was using air conditioning components during heating and cooling operation with both R12 and R134a as refrigerant.

3.2 Waste heat recovery systems

Yu and Chau [37] has written a paper about how waste heat in gasoline vehicles and hybrid electric vehicles can be used to generate electrical energy that can be used to charge the battery. This opens the possibilities of a longer range of the battery and charging the battery while driving. The energy from the combustion goes to vehicle operations, exhaust gas, friction and coolant. The paper introduces a new thermoelectric waste heat recovery system that uses MPPT (maximum power point tracking) as a control technique to maximize the power output. The TEG (thermoelectric generator) system improves the power consumption and can recover power up to 50 % of the power consumption of automotives electronics.

Yang [36] writes about the potential of waste heat recovery systems in automotives and how this will improve the fuel economy. The article discusses a number of TE (Thermoelectric) waste heat recovery system that has been developed and how they effect the electric load and fuel economy. The discussion sums up to that waste heat recovery systems has potential in significant improvements in fuel economy in both hybrid and conventional vehicles. The challenges are large scale production and finding thermodynamic material that is proper for the application.

Hsu et al. [24] has made experiments and simulations of a waste heat recovery system using TEG to recover heat to electrical energy. The waste heat was recovered from the exhaust gas and eight TEG was used. The results shows that recovery of heat decreases the consumption of petrolium. The properties of different TE material were also investigated.

3.3 Modelling and simulation of heat pumps

Modelling of heat pumps varies in the literature between models being deterministic or mathematical models. The case when the heat pump is constructed by four different components enables the possibility to have a mixture between the two types of modelling.

In the report Islam Mafizul and Salam Abdul [25] a PID and MPC controller for heating domestic water with a heat pump where developed. The system was modelled by system identification tool in MATLAB and a black box model was created from measured data.

In the report Baster Eric [9] a heat pump with air source implemented in a house with radiators is theoretical explained and modelled. The modelling is made according to IDEAS, which is a simplified way to model the dynamic approach of the heating system of buildings. The methodology is implemented as models in MATLAB Simulink to simulate the dynamic approach of the system. A general investigation of heat pump performance is made and is based on measurements on 30 heat pumps. A regression model for the COP was created. The radiator model and heating unit is developed by basic thermodynamic heat transfer. The heat transfer coefficient for the radiator is modelled by a regression tool and using manufactures data. The report also treats the sizing of conventional heating systems and sizing of heat pump systems. The model claims to simulate the power required by the air source heat pump depending on the temperature controller.

Badiali and Colombo [7] describes in a technical report how the dynamics of a heat pump with water and refrigerant as working fluids can be modelled in MATLAB Simulink. Each of the four components are separately described, modelled and finally merged into a heat pump Simulink model. The compressor is modelled as a reciprocating compressor with orifice equations for the inlet and outlet valve. The compression process is modelled as polytropic and also adiabatic if the polytropic constant is set to γ . The reciprocating compressor has a clearance volume and in this report this volume is taken into account. The dynamic approaches of the heat exchangers in the condenser and evaporator are modelled with a finite volume method. The finite volume method means that the heat exchanger in the condenser is divided into three parts depending on the phase of the refrigerant. The heat exchanger model contains governing mass balance and energy balance equations, which is discretized to each finite volume. The model has the assumptions that there is no pressure drops over the heat exchangers, neglected axial conduction, neglected shell capacitance and small tube conductivity. The expansion valve has a faster dynamic than the heat exchanger and is therefore modelled as a static component with constant enthalpy.

MacArthur [30] has developed a mathematical dynamical model of a heat pump. The model includes sub models of the condenser, evaporator, compressor, accumulator and expansion valve. The compressor is a reciprocating compressor and the compression is modelled as polytropic with suction and discharge pressure drops. The heat transferred through the wall is modelled with energy balance equations. The mass flow from the compressor is assumed to be polytropic and is computed with the polytropic equation. The heat exchanger is modelled with governing continuity and energy balance equations. The condenser is modelled with three discretized control volumes for the each fluid and the wall. The first volume contains only superheated vapor, the second a mix of vapor/liquid and the third only liquid. The evaporator is modelled in the same way but with two control volumes. This modelling gives a prediction of both the liquid and vapor flows in the condenser and evaporator. The expansion valved is modelled as both a fixed orifice and a thermodynamic expansion device. The system response

and response of each component is simulated in the report. The phase composition in the refrigerant due to transient behaviour is simulated and studied.

In Alotaibi et al. [5] a cross flow model of a heat exchanger is developed and the control ability is studied. The working medium is water that flows in a pipe and the cross flow air is exchanging heat with the water. In the work a finite numerical method is used to set up the equations of the convection and conduction between the air and the water. The dynamics of the system is modelled with partial differential equations. The model makes it possible to control the final states of the system. The study shows that the control ability is more difficult when having high water and air mass flows. An optimum of water mass flow rate for best control ability is found in the study.

Yamaguchi et al. [35] develops a simulation model for a CO₂ heat pump. The model is validated using an actual CO₂ heat pump water heater. The compressor is modelled with energy balance equations, and with volumetric efficiency, adiabatic efficiency and mechanical efficiency depending on the pressure ratio over the compressor. The heat exchanger is modelled by using continuity, energy balance and pressure drop equations. The pressure drop is modelled differently depending on if the refrigerant has a two phase flow or single phase flow. The heat transfer coefficient for the refrigerant is modelled after a flow pattern map where the flow is divided into six types of flow patterns. The expansion valve is modelled as a static component with constant enthalpy. The heat transfer performance and the pressure drop are taken into account. The effects of the inlet water temperature as well as the outside air temperature are studied. The inlet water temperature used in the study varied between 10-40° C while the outside air temperature differs between 13-28° C. The average difference in COP between simulation model and experiments is only 1.5 %.

In Domanski and Didion [12] an air source heat pump is modelled with analytically based components during steady state operations. The reciprocating hermetic compressor is modelled by the polytropic equation and by adding heat transfer equations for the compressor the heat transfer loss through the shell is taken into account. The heat transfer coefficient is modelled with respect to Nusselt number, Reynolds number and Prandtl number. The pressure drop over the compressor is caused by friction and dynamic effect. The pressure drop for the refrigerant is modelled for the inlet, suction process, discharge process and outlet. Constants for the pressure drop equations needs to be found by experimental investigation on a compressor. The expansion device is in detail modelled with constant flow which task is to maintain the pressure drop so that the refrigerant fully condenses over the condenser. The pressure drop over the expansion device depends on inlet friction loss and acceleration loss and is modelled by Bernoulli equation, equation of motion and continuity equation. The expansion device can be divided into two sections where the first section contains single phase flow and the second contains two phase flow. The same equations can be used for the two sections but for the liquid flow incompressible flow can be applied. Adia-

batic flow case is assumed in the model. The heat exchangers are modelled with energy balance equations and with respect to both subcooling and overheating. The heat transfer is modelled for the different cases at the inlet and outlet of the heat exchanger. This means that the refrigerant can be a mixture at the inlet and outlet and subcooled or overheated at the inlet and outlet. The heat transfer coefficient will differ depending on single or two phase flow in the heat exchangers. It will effect the flow pattern and further more effect the forced convection. The computer program for the heat pump is validated against laboratory data.

Fisher and Rice [17] models an air-to-air heat pump using two different compressor models. The first model is a reciprocating compressor using manufacturers data (compressor maps). The second one is a loss and efficiency-based compressor model (also a reciprocating compressor) which uses the internal energy balances when calculating the needed variables. The map-based compressor model uses empirical performance curves obtained from compressor measurements performed by the manufacturers. Compressor variables such as motor power input and refrigerant mass flow rate can be calculated using these performance curves. The compression is assumed to be isentropic and compressor shell losses are being taken into account. The condenser and evaporator models are assuming that the heat exchangers consists of equivalent, parallel refrigerant circuits with unmixed flow on both the air and refrigerant sides. The refrigerant side equations are divided into a superheated and a two-phase region for the evaporator and a superheated, a two-phased and a subcooled region for the condenser model. Air- and refrigerant-side pressure drops are taken into consideration and are calculated. The heat transfer coefficient is variable meaning that it changes depending on the flow and region inside the condenser/evaporator. Just like Domanski and Didion [12] the heat transfer coefficient is depending on the Reynolds number and the Prandtl number of the refrigerant but not on the Nusselt number. The computer program that were made by Fisher and Rice [17] contains subroutines for three different expansion devices: capillary tubes, thermostatic expansion valves (TXV) and short-tube orifices so that any of these can be modeled.

Gordon and Choon Ng [18] presents a thermodynamic chiller model based on the COP value. The COP value is determined by experimental data from 30 heat pumps with different cooling capacities between 30 - 1300 kW. The main objective of the investigation is to use the model for diagnosis of chillers. With thermodynamic heat transfer equation a governing chiller equation can be formed with respect to the value of COP. For each investigated chiller three constants are determined by linear regression and these constants where used to predict the performance. The result was compared with measured performance data.

Table 3.1 shows a summary of the different models.

Table 3.1: The table is a summary of the models found in the literature.

	Compressor	Heat exchanger	Expansion valve	Other
Islam Mafizul and Salam Abdul	-	-	-	Black box model. PID and MPC controller
Eric Baster	-	Heat transfer equations. Heat transfer coefficient regression model.	-	COP regression model.
Badiali and Colombo	Polytropic compression. Clearance volume.	Finite volume method. Mass and energy balance.	Static isenthalpic.	
MacArthur	Polytropic compression. Suction and discharge pressure drops. Shell loss.	Discretized control volumes.	Fixed orifice and TXV.	System response simulated.
Alotabi et al.	-	Cross flow. Finite numerical method. PDE:s	-	Control ability of heat exchangers
Yamaguchi et al.	Energy balance and efficiency.	Continuity, energy balance and pressure drop equations. Heat transfer coefficient modelled by flow pattern.	Static isenthalpic.	
Domanski and Didion	Polytropic compression. Shell loss. Variable heat transfer coefficient. Pressure drop.	Energy balance with sub-cooling and overheating. Variable heat transfer coefficient.	Detailed modelled with constant flow. Adiabatic.	Steady state operations
Fisher and Rice	Compressor maps. Loss and efficiency model. Isentropic compression. Shell loss.	Subcool and superheated. Pressure drop. Variable heat transfer coefficient.	Capillary tubes, TXV, short-tube orifices	
Gordon and Choong Ng	-	-	-	COP linear regression model.

3.4 Two phase flow

Two phase flow will occur in the evaporator and condenser. A phase mixture of liquid and vapor will occur at the inlet of the evaporator and at the outlet there will be a mixture, saturated vapor or overheated vapor. The refrigerant will be overheated vapor at the inlet of the condenser and saturated or undercooled liquid at the outlet. This phase change over the evaporator and condenser will create a two phase flow which needs to be taken into account when modelling a heat pump. The two phase flow will affect the heat transfer coefficient of the refrigerant. Depending on if there is a one phase or two phase flow, which both occur in the evaporator and condenser, the heat transfer coefficient will change. Along with the length of the condenser the flow pattern will change from vapor and annular flow, to slug, plug, bubbly and liquid flow. In slug there are larger vapor parts in the liquid and the vapor/liquid composition will change until the phase is only liquid. There will be smaller and smaller bubbles along the length of the condenser.

For the region for saturated/overheated vapor and saturated/undercooled liquid the refrigerant will have a one phase flow. In Erhard et al. [16] and Badiali and Colombo [7] the heat transfer coefficient of single phase flow is modelled by the Dittus-Boelter correlation for turbulent flow. For laminar flow the Sieder-Tate correlation is used. These equations are dependant of the Nussel, Prandtl and Reynolds numbers of the flow. The two phase flow is simple modelled by a two phase multiplier. In Santa [34] there are several methods discussed for modelling the two phase flow heat transfer coefficient where the two phase multiplier method is discussed. Cavallini Zecchini's correlation is one of the methods discussed which is similar to Dittus Boelter for turbulent one phase flow and with incomplete condensation. The two phase flow is modelled with an equivalent Reynolds number. This method of modelling is semi-empirical and adapted for annular flow. Travis et al. is another method discussed which uses a parameter called Lockhart-Martinelli to take the incomplete condensation into account. Next method discussed is Shah's correlation which also takes the mixture quality and pressure into account. This model is formed as Dittus Boelter but with an additional term and is adapted for annular flow regimes. Akers, Dean, Collier correlation is adapted to when the pipe length is very long or when the rate of condensation is very large. This method is also similar to Dittus-Boelter. Further on this method does not depend on the temperature difference, is adapted to annular flow and are sometimes overestimated. Boyko & Kruzhilin is a method which takes density of two phase, heat transfer coefficient in one phase and vapor quality into account. The method has a restricted range where it can be used which is between 1500 and 15000 in Reynolds number and is adapted to annular flow regimes. The last studied method is Dobson et al. correlation which takes wavy flow into account and operates in annular flow regimes. There are several ways of modelling the two phase and single phase heat transfer coefficient and there is a need of finding one method that is most suitable to the given application.

4

Models

4.1 System overview

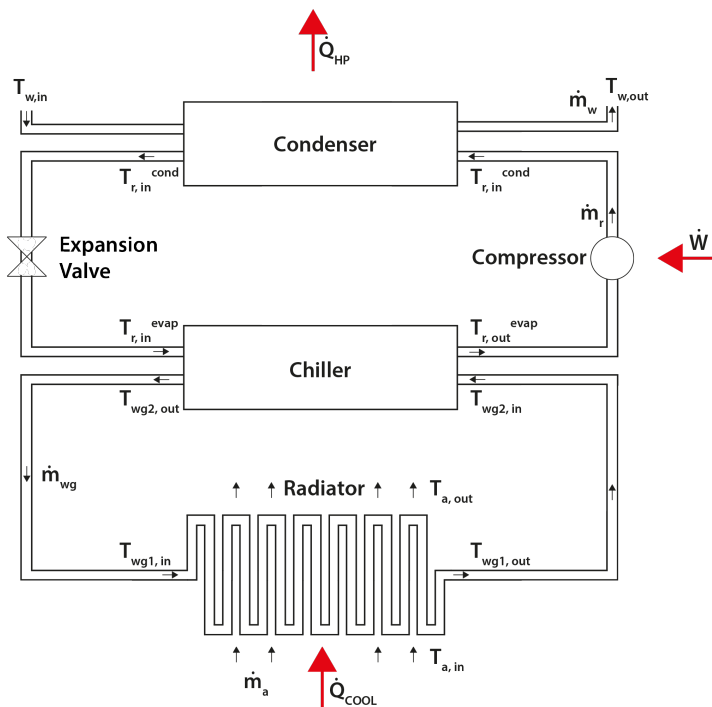


Figure 4.1: System overview.

The complete system can be seen in figure 4.1. The heat is transferred via a radiator from either ambient air or waste heat from different vehicle components to a water/glycol mixture. The water/glycol mixture then enters the **chiller** where heat is transferred to the refrigerant. The energy transfer from air to refrigerant therefore consists of two heat transfers instead of one. One between the air and the water/glycol mixture and another one between the water/glycol mixture and the refrigerant.

In the condenser, heat is then transferred from the hot refrigerant to a water tube. The water is then transported to the areas inside the vehicle where heat is needed. Counter flow is assumed in both condenser and chiller.

4.2 Working medium

In this report there are several fluids/gases, such as refrigerant, water, water/glycol-mixture and air, acting as working medium. These fluids/gases has different properties depending on the pressure and temperature. The properties is collected in a map and a function called f_{map} is used to find the correct values for all the different parameters mentioned below, the function has temperature and pressure as input. The refrigerant is the only working medium that will change phase and have two phase flow during the heat pump working process. The water, water/glycol-mixture and air will have a one phase flow.

During condensation and evaporation the refrigerant will change phase. The saturating values of the enthalpy, density, and specific volume is depending on the pressure during the processes.

$$h_L^{sat} = f_{map}(p) \qquad h_V^{sat} = f_{map}(p)$$

$$\rho_L^{sat} = f_{map}(p) \qquad \rho_V^{sat} = f_{map}(p)$$

$$\vartheta_L^{sat} = f_{map}(p) \qquad \vartheta_V^{sat} = f_{map}(p)$$

The specific heat capacity during a constant volume process is also depending on the pressure during the phase change, but when the refrigerant is overheated or subcooled the value of c_v will also depend on the temperature. Therefore the function has two inputs to describe the properties of c_v when overheating or subcooling appears.

$$c_{v,L}^{sat} = f_{map}(p) \qquad c_{v,V}^{sat} = f_{map}(p) \qquad c_v = f_{map}(T, p)$$

The same conditions as for c_v applies for the specific heat capacity during constant pressure.

$$c_{p,L}^{sat} = f_{map}(p) \quad c_{p,V}^{sat} = f_{map}(p) \quad c_p = f_{map}(T, p)$$

The boiling/evaporating and condensing temperature is depending on the pressure during the phase change.

$$T_{evap} = f_{map}(p)$$

$$T_{cond} = f_{map}(p)$$

The equations for the condenser and evaporator is depending on some refrigerant derivatives, which can be calculated with the map function. The following derivatives are mapped:

$$\frac{d\rho_{3,cond}}{dp_{cond}} = f_{map}(p, T) \quad \frac{d\rho_V^{sat}}{dp_{cond}} = f_{map}(p) \quad \frac{d\rho_L^{sat}}{dp_{cond}} = f_{map}(p)$$

$$\frac{dh_L^{sat}}{dp_{cond}} = f_{map}(p) \quad \frac{d\rho_V^{sat}}{dp_{evap}} = f_{map}(p) \quad \frac{d\rho_L^{sat}}{dp_{evap}} = f_{map}(p)$$

For the water, water/glycol-mixture and air there is a need to describe the one phase flow parameters. Therefore the heat transfer coefficient, heat conductivity and dynamic viscosity is mapped. The inputs to the map are temperature and pressure while the fluids and gas is continuous to have a one phase flow with no phase changes.

$$k = f_{map}(T, p)$$

$$\mu = f_{map}(T, p)$$

Data for each working medium is collected from National Institute of Standards and Technology [31] and from Honeywell refrigerants [21]. The properties of the water/glycol fluid is provided from The Dow Chemical Company [10]. The function f_{map} interpolates for the desired input parameters which in temperature and pressure. The pressure and temperature are coupled for the saturation properties and therefore is only one of the input parameters needed to determine the output value.

4.3 Compressor

The compressor is modelled as an isotropic component. The following assumption can be drawn for the compressor:

- Since the compressor is modelled as isentropic there is no heat exchange with the surroundings and the process is reversible.
- The volumetric efficiency is set to be constant for different speeds.

The mass flow in the compressor is related to how much volume the compressor theoretically can obtain during the suction process. Depending on the density of the refrigerant and the speed of the compressor the theoretically mass flow can be determined. The volume of refrigerant compressed into the compressor is less than the theoretically which means that the compressor has a volumetric efficiency. Therefore the mass flow rate from the compressor is defined as:

$$\dot{m} = \rho_{suc} \eta_{vol} V_{suc} \frac{N}{60} \quad (4.1)$$

where ρ_{suc} is the density at the compressor inlet, η_{vol} is the volumetric efficiency, N is the compressor speed and V_{suc} suction volume.

The process over the compressor is ideally isentropic which means that the process is adiabatic and reversible. There is no heat exchange with the surroundings and the direction of the process can be reversed.

The compression stage can be expressed in form of a polytropic process. The pressure and volume relates to each other in the following way for an ideal gas during the isentropic compression:

$$pV^n = constant \quad (4.2)$$

The polytropic exponent n depends on which process that occurs. If $n = 1$ the process is isotherm, $n = 0$ the process is isobar, if $n \rightarrow \infty$ the process is isochor and if $n = \gamma$ the process is adiabatic. γ describes how the temperatures and pressures before and after the compression relates to each other, which also can be expressed as the ratio between c_p and c_v for an ideal gas. The ideal gas law is expressed as:

$$pV = mRT \quad (4.3)$$

Combining the polytropic process equation 4.2 with the ideal gas law equation 4.3 the following expression for the temperature ratio is found:

$$\frac{T_2}{T_1} = \left(\frac{p_2}{p_1}\right)^{\frac{\gamma-1}{\gamma}} \quad (4.4)$$

The vapour quality before the compressor is depending on how near the enthalpy at the compressor inlet is the saturated value of the enthalpy. The following equation is used to calculate the quality, x :

$$h_1 = x \cdot h_V^{sat} + (1 - x) \cdot h_L^{sat} \quad (4.5)$$

Where h_V^{sat} is the vapor saturated enthalpy value and h_L^{sat} is the liquid saturated enthalpy value. The content of steam can be used to determine the density. The following equation is used to determine the density before the compressor:

$$\rho_{suc} = \frac{\rho_L \cdot \rho_V}{x \cdot \rho_L + (1 - x) \cdot \rho_V} \quad (4.6)$$

Where ρ_L is the liquid saturated density value and ρ_V is the vapor saturated density value.

To calculate the enthalpy after the compressor (h_2), the specific volume (ϑ_2) and the polytropic work (W_{pol}) has to be calculated:

$$\vartheta_2 = \left(\frac{p_1 \vartheta_1^n}{p_2} \right)^{1/n} \quad (4.7)$$

where $n = \gamma$ for a polytropic process.

$$W_{pol} = \frac{n}{n-1} (p_2 \vartheta_2 - p_1 \vartheta_1) \quad (4.8)$$

$$h_2 = \frac{W_{pol}}{\eta_{pol}} + h_1 \quad (4.9)$$

where η_{pol} is the polytropic efficiency.

According to the first law of thermodynamics the power consumption over the compressor can be expressed as:

$$\dot{W} = \dot{m}(h_2 - h_1) \quad (4.10)$$

4.4 Condenser

The condenser modelled in this report is a counter flow water condenser. This means that the refrigerant transfers heat to water inside a pipe with a flow in the opposite direction compared to the refrigerant. Since the refrigerant goes from superheated vapour, to liquid/vapour mixture, to liquid the condenser has been divided into three zones to better describe the refrigerant properties.

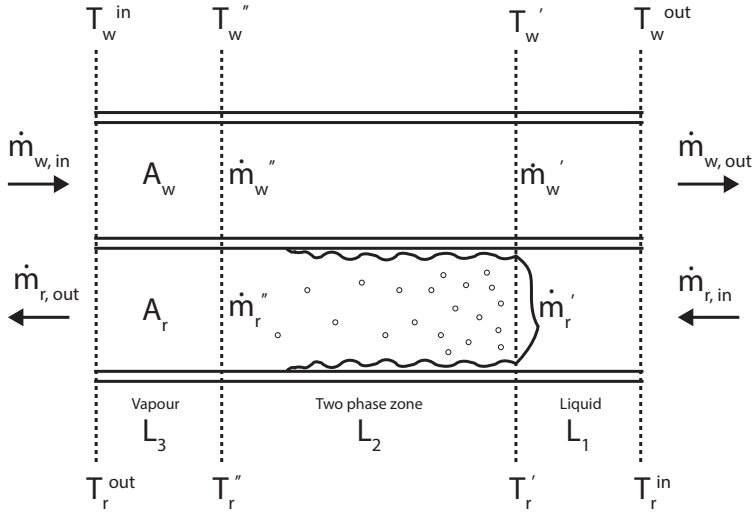


Figure 4.2: Figure showing the three different zones that occur during the condensing process.

When modelling the condenser there are a few assumptions made to simplify the modelling:

- The walls of the condenser are assumed to be thin and the heat exchange are therefore transmitted between the refrigerant and water by convection.
- The condenser are assumed to be formed as a circular pipe with a constant area through out the whole condenser.
- There is no pressure drop over the condenser.
- Axial heat conduction is negligible.
- Kinetic energy is negligible.
- It is assumed that the condensation is complete.

Refrigerant side energy equations

Andersson and Jerregård [6] describes the basic equations for refrigeration systems. By using the energy balance expressed in equation 2.16 the following expression describes the energy balance:

$$A_{c,cond} dz \left(\frac{d\rho_{cond}}{dt} h_{cond} + \frac{dh_{cond}}{dt} \rho_{cond} - \frac{dp_{cond}}{dt} \right) = \dot{m}_{in} h_{in} - \dot{m}_{out} h_{out} + \alpha_{cond} \pi d_r dz (T_{w,c} - T_{r,c}) \quad (4.11)$$

Where h_c is the enthalpy in the control volume, A_c is the cross-sectional area, dz is the elemental length, ρ_c is the density, p_{cond} is the condensing pressure, d_r is the diameter, \dot{m}_{in} and \dot{m}_{out} is the massflow into and out from the control volume, h_{in} and h_{out} is the enthalpy into and out of the control volume. $T_{w,c}$ and $T_{r,c}$ is the temperatures in the control volume on the water side and refrigerant side of the condenser.

When assuming that the condensation is complete this means that the enthalpy out of the first zone and out of the second zone is set to saturation values for the current condensing pressure.

$$h' = h_V^{sat} \quad (4.12)$$

$$h'' = h_L^{sat} \quad (4.13)$$

Integrating the equation 4.11 for the third zone of the condenser results in the following equation:

$$A_{c,cond}L_3\left(\frac{d\rho_{3,cond}}{dt}h_{3,cond} + \frac{dh_{3,cond}}{dt}\rho_{3,cond} - \frac{dp_{cond}}{dt}\right) = \quad (4.14)$$

$$\dot{m}''h'' - \dot{m}_{out}h_{out} + \alpha_{3,cond}\pi d_r L_3(T_{w3,cond} - T_{r3,cond})$$

Where ρ_{3c} is the mean value of the density in the third zone, h_{3c} is the mean value of the enthalpy in the third zone, \dot{m}'' is the massflow into the third zone, α_3 is the heat transfer coefficient in the third zone and h'' is the enthalpy into the third zone.

The derivatives of the density and enthalpy can be rewritten using the chain rule:

$$A_{c,cond}L_3\left(\frac{d\rho_{3,cond}}{dp_{cond}}\frac{dp_{cond}}{dt}h_{3,cond} + \frac{dh_{3,cond}}{dt}\rho_{3,cond} - \frac{dp_{cond}}{dt}\right) = \quad (4.15)$$

$$\dot{m}''h'' - \dot{m}_{out}h_{out} + \alpha_{3,cond}\pi d_r L_3(T_{w3,cond} - T_{r3,cond})$$

The massflow into the third zone is assumed to be equal to the massflow out of the third zone. The mean value of ρ_c and h_c can be expressed with the following equations for the third zone:

$$\rho_{3,cond} = \frac{1}{2}(\rho_L^{sat} + \rho_{out}) \quad (4.16)$$

$$h_{3,cond} = \frac{1}{2}(h_L^{sat} + h_{out}) \quad (4.17)$$

The final enthalpy out of the condenser is expressed with the following equation:

$$\frac{dh_{out}}{dt} = \frac{2}{\rho_{3,cond}} \left(\frac{1}{A_{c,cond} L_3} (\dot{m}_{out}(h_L^{sat} - h_{out}) + \alpha_{3,cond} \pi d_r L_3 (T_{w3,cond} - T_{r3,cond})) - h_{3,cond} \frac{d\rho_{3,cond}}{dp_{cond}} \frac{dp_{cond}}{dt} + \frac{dp_{cond}}{dt} \right) - \frac{dh_L^{sat}}{dt} \quad (4.18)$$

The temperatures $T_{w3,cond}$ and $T_{r3,cond}$ is the mean temperatures in the third zone on the water side and on the refrigerant side of the condenser.

Refrigerant side mass equations

The conservation of mass in the condenser is expressed according to equation 2.17. This equation can be rewritten to:

$$A_{c,cond} L_{cond} \frac{d\rho_{cond}}{dt} = \dot{m}_{in} - \dot{m}_{out} \quad (4.19)$$

Since the massflow into and out of the first and third zone is set to constant the following equation for the pressure in the second zone can be expressed:

$$\frac{dp_{cond}}{dt} = \frac{\dot{m}_{in} - \dot{m}_{out}}{A_{c,cond} L_{2,cond} \frac{d\rho_{2,cond}}{dt}} \quad (4.20)$$

The mean density of the second zone of the condenser can be expressed with the following equation:

$$\rho_{2,cond} = \rho_V^{sat} x_{mean,cond} + \rho_L^{sat} (1 - x_{mean,cond}) \quad (4.21)$$

Where $x_{mean,cond}$ is the mean vapour quality for the second zone of the condenser. The derivative of the mean density in the second zone can be expressed with the following equation:

$$\frac{d\rho_{2,cond}}{dt} = \left(\frac{d\rho_V^{sat}}{dp_{cond}} x_{mean,cond} + \frac{d\rho_L^{sat}}{dp_{cond}} (1 - x_{mean,cond}) \right) \frac{dp_{cond}}{dt} \quad (4.22)$$

The derivatives $\frac{d\rho_V^{sat}}{dp_{cond}}$ and $\frac{d\rho_L^{sat}}{dp_{cond}}$ is specific for the refrigerant and is maintained by the map function.

Water side energy equations

According to The energy balance for the water side can be written as[7]:

$$\frac{\partial T_w}{\partial t} A_{c,w} \rho_w c_{p,w} = \pi d_w \alpha_w (T_r - T_w) - \dot{m}_w c_{p,w} \frac{\partial T_w}{\partial z} \quad (4.23)$$

where $A_{c,w}$ is the cross sectional area, dz is the length element of the heat exchanger, $c_{p,w}$ is the specific heat capacity of water, ρ_w is the density of the water, d_w is the diameter and α_w is the heat transfer coefficient of the water. The temperatures T_r^{out} and T_w^{out} is the out temperatures on the refrigerant side and water side of the condenser. The mass flow of the water is defined as \dot{m}_w .

Discretizing the partial derivative with respect to space using equation 4.24:

$$\frac{\partial(T)}{\partial z} = \frac{T_w(i) - T_w(i-1)}{dz} \quad (4.24)$$

equation 4.23 for the i :th node becomes:

$$\frac{dT_w(i)}{dt} = \frac{1}{A_{c,w}\rho_w c_{p,w}} [\pi d_w \alpha_w (T_r(i) - T_w(i)) - \frac{\dot{m}_w c_{p,w}}{dz} (T_w(i) - T_w(i-1))] \quad (4.25)$$

Thereby the water temperature equations for each zone becomes:

$$\frac{dT_w''}{dt} = \frac{1}{A_{c,w}\rho_w c_{p,w}} [\pi d_w \alpha_{w3} (T_r'' - T_w'') - \frac{\dot{m}_w c_{p,w}}{L_3} (T_w'' - T_{w,in})] \quad (4.26)$$

$$\frac{dT_w'}{dt} = \frac{1}{A_{c,w}\rho_w c_{p,w}} [\pi d_w \alpha_{w2} (T_r' - T_w') - \frac{\dot{m}_w c_{p,w}}{L_2} (T_w' - T_w'')] \quad (4.27)$$

$$\frac{dT_{w,out}}{dt} = \frac{1}{A_{c,w}\rho_w c_{p,w}} [\pi d_w \alpha_{w1} (T_{r,in} - T_{w,out}) - \frac{\dot{m}_w c_{p,w}}{L_1} (T_{w,out} - T_w)] \quad (4.28)$$

The heat transfer coefficient of water α is dependent on the conditions of the water and is calculated using the Dittus-Boelter equation, see eq. 4.29.

$$Nu = \frac{\alpha d}{k} = 0.023 Re^{0.8} Pr^n \quad (4.29)$$

where $n = 0.4$ since the water is heated. The Reynolds number and Prandtl number are calculated using equations 4.30 and 4.31.

$$Re = \frac{\rho v d}{\mu} \quad (4.30)$$

$$Pr = \frac{c_p \mu}{k} \quad (4.31)$$

The temperature difference between the refrigerant and the water for each zone can be expressed with a mean temperature difference according to equation 2.28:

$$\Delta T_{1,cond} = \frac{1}{2} (T_r' + T_{r,in}) - \frac{1}{2} (T_w' + T_{w,out}) \quad (4.32)$$

$$\Delta T_{2,cond} = \frac{1}{2} (T_r'' + T_r') - \frac{1}{2} (T_w'' + T_w') \quad (4.33)$$

$$\Delta T_{3,cond} = \frac{1}{2}(T_r'' + T_{r,out}) - \frac{1}{2}(T_w'' + T_{w,in}) \quad (4.34)$$

The final expressions for the enthalpy of the water can now be written as:

$$\frac{dT_w''}{dt} = \frac{1}{A_{c,w}L_3\rho_w c_{p,w}} [\pi d_w L_3 \alpha_{w3} \Delta T_{3,cond} - \dot{m}_w c_{p,w} (T_w'' - T_{w,in})] \quad (4.35)$$

$$\frac{dT_w'}{dt} = \frac{1}{A_{c,w}L_2\rho_w c_{p,w}} [\pi d_w L_2 \alpha_{w2} \Delta T_{2,cond} - \dot{m}_w c_{p,w} (T_w' - T_w'')] \quad (4.36)$$

$$\frac{dT_{w,out}}{dt} = \frac{1}{A_{c,w}L_1\rho_w c_{p,w}} [\pi d_w L_1 \alpha_{w1} \Delta T_{1,cond} - \dot{m}_w c_{p,w} (T_{w,out} - T_w)] \quad (4.37)$$

4.5 Evaporator

In the evaporator side of the heat pump the outside air transfers heat to the refrigerant by using a cross flow heat exchanger. The refrigerant is a vapour/liquid mixture at the input and vapour, or vapour/liquid mixture, at the output. Even if the refrigerant is fully evaporated inside the evaporator the vapour zone will be a lot smaller compared to the mixture zone. Therefore the evaporator is modelled as a one-zone heat exchanger. The assumptions made for the condenser is also valid for the evaporator. The evaporation is fully or partly complete depending on the enthalpy out.

Refrigerant side energy equations

The energy balance for the evaporator can when integrating the equation 2.16 be expressed as:

$$A_{c,evap} L_{evap} \left(\frac{d\rho_{evap}}{dt} h_{evap} + \frac{dh_{evap}}{dt} \rho_{evap} - \frac{dp_{evap}}{dt} \right) = \quad (4.38)$$

$$\dot{m}_{in} h_{in} - \dot{m}_{out} h_{out} + \alpha_{evap} \pi d_r L_{evap} (T_{w,evap} - T_{r,evap})$$

Where L_{evap} is the length of the evaporator, ρ_{evap} is the density of the evaporator control volume, h_{evap} is the enthalpy of the control volume. The density and enthalpy of the evaporator control volume can be expressed with the following mean values:

$$\rho_{evap} = \rho_V^{sat} x_{mean,evap} + \rho_L^{sat} (1 - x_{mean,evap}) \quad (4.39)$$

$$h_{evap} = \frac{1}{2}(h_{in} + h_{out}) \quad (4.40)$$

Where $x_{mean,evap}$ is the mean vapour quality. By deriving the mean value equations for the density and enthalpy the following expressions can be expressed for the derivatives:

$$\frac{d\rho_{evap}}{dt} = \left(\frac{d\rho_V^{sat}}{dp_{evap}} x_{mean,evap} + \frac{d\rho_L^{sat}}{dp_{evap}} (1 - x_{mean,evap}) \right) \frac{dp_{evap}}{dt} \quad (4.41)$$

$$\frac{dh_{evap}}{dt} = \frac{d(h_{in} + h_{out})}{dt} \quad (4.42)$$

Where the derivatives $\frac{d\rho_V^{sat}}{dp_{evap}}$, $\frac{d\rho_L^{sat}}{dp_{evap}}$ are values found in the map function and are specific for the refrigerant. By introducing a simplified expression for the heat capacity of the heat exchanger as a constant heat rate per difference in mean temperature between both fluids [W/K] the following equation is obtained:

$$\Psi_{evap} = constant \quad (4.43)$$

The mean temperature difference of the evaporator can be expressed with the following equation:

$$\Delta T_{evap} = \frac{1}{2}(T_{a,in} + T_{a,out}) - \frac{1}{2}(T_{r,in} + T_{r,out}) \quad (4.44)$$

The equations 4.44, 4.43 together with the energy balance gives the following final equation for the enthalpy out of the evaporator:

$$\frac{dh_{out}}{dt} = \frac{2}{\rho_{evap}} \left(\frac{1}{A_{c,evap} L_{evap}} (\dot{m}_{in} h_{in} - \dot{m}_{out} h_{out} + \right. \quad (4.45)$$

$$\left. \Psi_{evap} \Delta T_{evap}) - \frac{d\rho_{evap}}{dt} \left(\frac{h_{in} + h_{out}}{2} \right) + \frac{dp_{evap}}{dt} \right) - \frac{dh_{in}}{dt}$$

Where $\frac{d\rho_{evap}}{dt}$ is expressed with equation 4.41.

Refrigerant side mass equations

The conservation of mass can for the evaporator be expressed in the same way as for the condenser. The mass balance becomes:

$$A_{c,evap} L_{evap} \frac{d\rho_{evap}}{dt} = \dot{m}_{in} - \dot{m}_{out} \quad (4.46)$$

The pressure can then be expressed with the following differential equation:

$$\frac{dp_{evap}}{dt} = \frac{\dot{m}_{in} - \dot{m}_{out}}{A_{c,evap} L_{evap} \frac{d\rho_{evap}}{dt}} \quad (4.47)$$

Where the derivative of the density is calculated with equation 4.41.

4.5.1 Chiller

When the chiller is introduced a loop containing a water/glycol mixture is placed between the outside air and the refrigerant. The open air transfers heat to the water/glycol mixture using cross flow and the mixture in turn transfers the energy to the refrigerant using counter flow.

The air side equation can be written as:

$$\frac{dT_a^{out}}{dt} = \frac{1}{\rho_a c_{p,a} A_a L_a} (\dot{m}_a c_{p,a} (T_a^{in} - T_a^{out}) - \alpha_a \pi d_a L_a \Delta T_{rad}) \quad (4.48)$$

Where ΔT_{rad} can be written as:

$$\Delta T_{rad} = \frac{1}{2} (T_a^{in} + T_a^{out}) - \frac{1}{2} (T_{wg1} + T_{wg1}^{out}) \quad (4.49)$$

The water/glycol side equation can be written as:

$$\frac{dT_{wg1}^{out}}{dt} = \frac{1}{\rho_{wg} c_{p,wg} A_{c,wg} L_{wg}} (\dot{m}_{wg} c_{p,wg} (T_{wg1}^{in} - T_{wg1}^{out}) + \alpha_{wg1} \pi d_{wg1} L_{wg1} \Delta T_{rad}) \quad (4.50)$$

The water/glycol side equation inside the chiller can be written as:

$$\frac{dT_{wg2}^{out}}{dt} = \frac{1}{\rho_{wg} c_{p,wg} A_{c,wg} L_{wg}} (\dot{m}_{wg} c_{p,wg} (T_{wg2}^{in} - T_{wg2}^{out}) - \alpha_{wg2} \pi d_{wg2} L_{wg2} \Delta T_{evap}) \quad (4.51)$$

Where:

$$\Delta T_{evap} = \frac{1}{2} (T_{wg2}^{in} + T_{wg2}^{out}) - \frac{1}{2} (T_r^{in} + T_r^{out}) \quad (4.52)$$

The heat transfer coefficient for the water/glycol fluid can be calculated in the same way as for the water in the condenser. Equation 4.45 is used for calculating the enthalpy of the refrigerant. By using the simplification Ψ_{evap} (see equation 4.43) the final expression for T_{wg1}^{out} can be written as:

$$\frac{dT_{wg2}^{out}}{dt} = \frac{1}{\rho_{wg} c_{p,wg} A_{c,wg} L_{wg}} (\dot{m}_{wg} c_{p,wg} (T_{wg2}^{in} - T_{wg2}^{out}) - \Psi_{evap} \Delta T_{evap}) \quad (4.53)$$

4.6 Expansion Valve

The dynamic response of the expansion valve is much faster compared to the heat exchangers. Therefore the expansion valve is modelled as a static component. The following assumptions are made for the expansion valve:

- There is no heat exchange with the surroundings and no energy losses over the expansion valve.
- The expansion valve is assumed to be isenthalpic.

According to Badiali and Colombo [7] the mass flow rate through the valve can be written as:

$$\dot{m} = \rho A_{EXV} C_{EXV} \sqrt{\frac{2}{\rho} (p_{cond} - p_{evap})} \quad (4.54)$$

where A_{EXV} is the cross sectional area and C_{EXV} is the flow coefficient of the orifice.

The expansion process is considered to be isenthalpic which means that the enthalpy is constant during the process, see equation 4.55.

$$h_4 = h_3 \quad (4.55)$$

4.7 Simulink model

This section describes the simulation approach and the simulink model results. A whole assembly of all the HP components is made in MATLAB Simulink.

Complete model

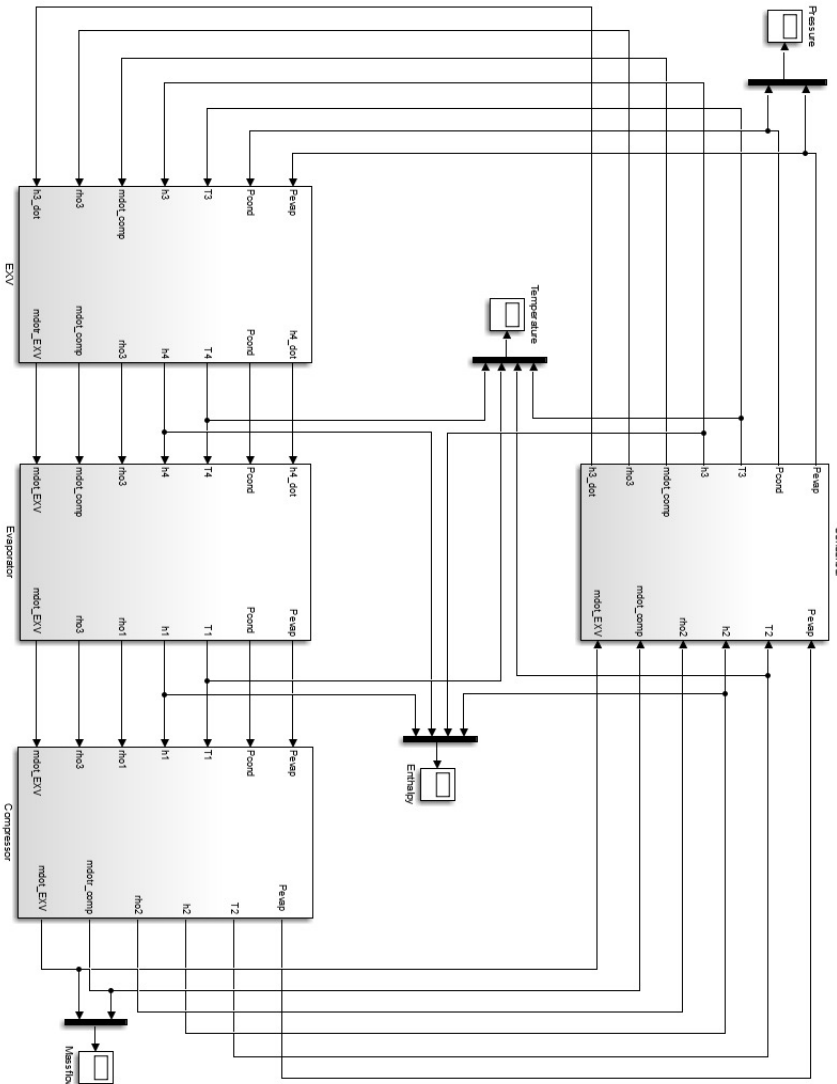


Figure 4.3: Figure showing the Simulink model of the HP system.

In figure 4.3 the structure of the Simulink model is shown. The simulation model includes the assembly of the HP components described earlier in this chapter. The input and output to each simulation component is condensing pressure, evaporating pressure, temperature, enthalpy, mass flow through the expansion device and mass flow created by the compressor. Also some components require density and the derivative of the enthalpy. The evaporator component includes the heat exchange with the water/glycol fluid in the chiller and the heat exchange with the surrounding air. The condenser component includes the heat exchange with the water.

A simple P-controller was used to produce the results presented in this report. The controller changed the expansion valve area to get the preferred vapour quality.

Simulation Issues

The density equation 4.6 caused problems with the simulation and therefore the density at the compressor inlet ρ_{suc} was calculated as a linear function of vapour quality between $x = 0.8$ and $x = 1.0$ where equation 4.6 is close to linear.

When using the controller it is very important that the initial condition on the evaporator is set as close to the stationary point as possible. If the difference is too large the condenser pressure can become unreasonably high/low.

5

Results

5.1 Map function results

The following plots shows the results when using the map-function for the different refrigerants. In the plot properties for the two refrigerants, R134a and R1234yf, is shown. The first plot below shows how the enthalpy for saturated vapour and liquid changes with pressures.

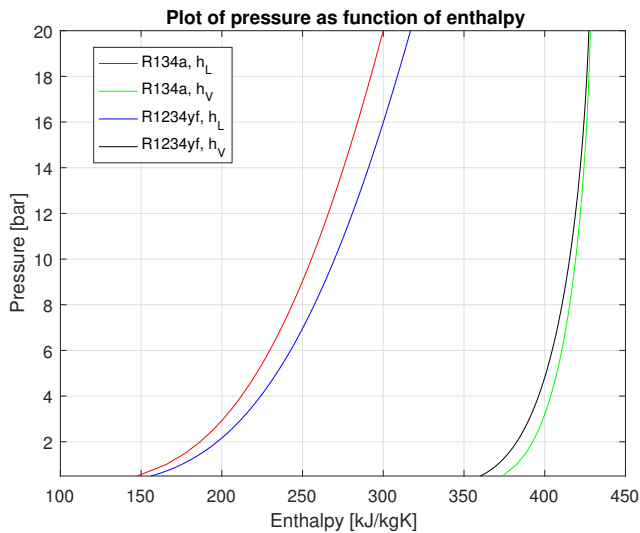


Figure 5.1: Figure showing the enthalpy for the refrigerants.

Further on figure 5.2 shows the density for saturated vapour and liquid for different pressures.

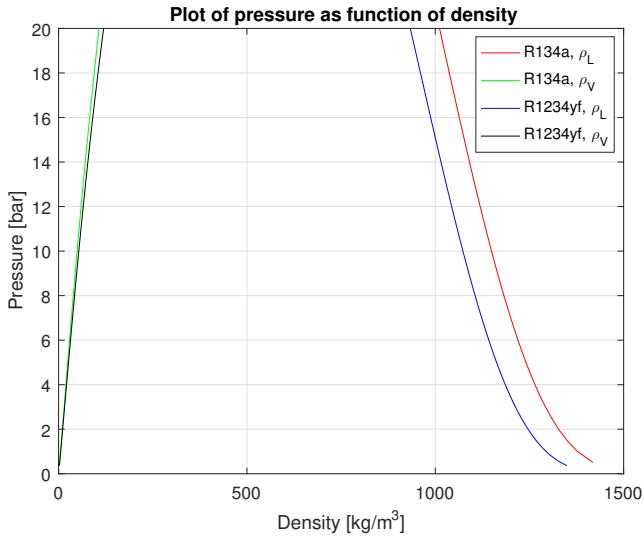


Figure 5.2: Figure showing the density for the refrigerants.

Plots for all other fluid properties from the map function can be seen in Appendix A.

5.2 Modelling and simulation results

This section shows the results from running the simulation during a certain setup and a selected refrigerant. The two refrigerant investigated are R134a and R1234yf. The simulations are made for different speeds and Ψ . Also tests are made to increase the output heating power from the condenser. When running a simulation the outside air temperature is set to 0°C and the speed is hold constant while the expansion valve area is changed to achieve different vapour qualities. Also a step in speed is made to study the dynamic of the system.

5.2.1 R134a

The results from running simulations for R134a is shown below. The simulations are evaluated for different speeds and different Ψ_{evap} , and also an investigating to achieve a high Q_{HP} is made.

The table below shows the results when running a simulation with reference speed of the compressor and the baseline value for the chiller[W/K].

Table 5.1: Table showing the simulation values for R134a with reference speed of the compressor and the baseline value for the chiller[W/K].

x	1	0.95	0.9	0.85	0.8
$A_{EXV} [mm^2]$	0.13	0.14	0.15	0.16	0.17
$h_1 [kJ/kg]$	398	388	378	368	358
$h_2 [kJ/kg]$	476	461	446	432	418
$h_3 [kJ/kg]$	249	250	251	251	252
$h_4 [kJ/kg]$	249	250	251	251	252
$\dot{m} [kg/s]$	0.0053	0.0056	0.0058	0.0061	0.0064
$p_{cond} [bar]$	14.8	14.6	14.3	14.0	13.7
$p_{evap} [bar]$	2.79	2.79	2.80	2.80	2.81
$\dot{Q}_{HP} [W]$	1194	1172	1145	1112	1073
$\dot{Q}_{COOL} [W]$	785	767	744	717	685
$\dot{W}_{comp} [W]$	409	405	401	395	388
$COP_{HP} [-]$	2.92	2.89	2.86	2.81	2.76
$COP_{COOL} [-]$	1.92	1.89	1.86	1.81	1.76

The values for the enthalpy and pressure in table 5.1 can be plotted to visualize the compressor cycle, which is shown in the figure below.

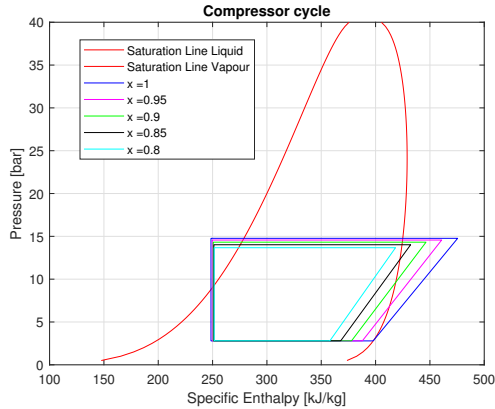


Figure 5.3: Figure showing the compressor cycle with reference speed of the compressor and the baseline value for the chiller[W/K].

Figure 5.3 shows how the vapour quality effects the compressor cycle. When the quality decreases in value the pressure on high side decreases and low pressure side increases. Also the slope between h_1 and h_2 (enthalpies before and after the compressor) increases with the quality. The values for \dot{Q}_{HP} in table 5.1 can be plotted against the vapour quality, which is shown in the figure below.

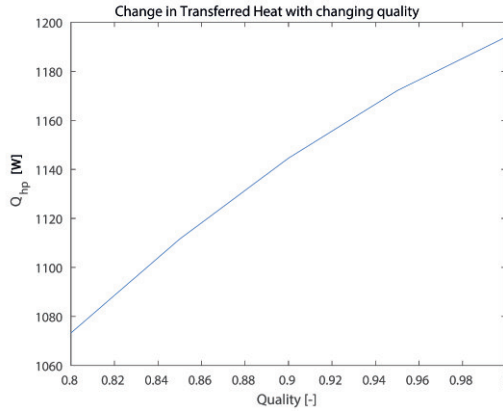


Figure 5.4: Figure showing how Q_{HP} changes for different vapour qualities x , with reference speed of the compressor and the baseline value for the chiller[W/K].

The figure shows how Q_{HP} decreases when decreasing the vapour quality. The value for COP_{HP} can also be plotted against the vapour quality, which is shown in the figure below.

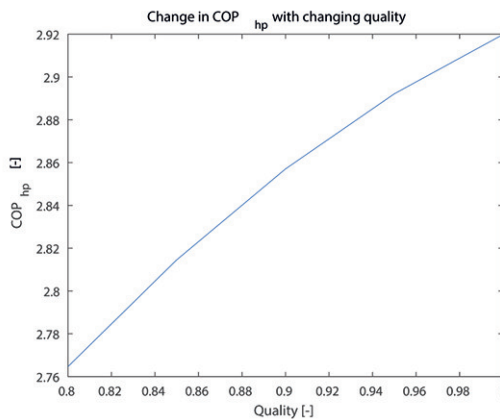


Figure 5.5: Figure showing COP_{HP} for different vapour qualities x , with reference speed of the compressor and the baseline value for the chiller[W/K].

The value of COP_{HP} also decreases in the same way as for Q_{HP} . The table below shows the results when running a simulation with with twice the reference speed of the compressor and the baseline value for the chiller[W/K].

Table 5.2: Table showing the simulation values for R134a with twice the reference speed of the compressor and the baseline value for the chiller[W/K].

x	1	0.95	0.9	0.85	0.8
A_{EXV} [mm ²]	0.26	0.28	0.30	0.32	0.35
h_1 [kJ/kg]	397	387	377	367	357
h_2 [kJ/kg]	476	461	446	431	416
h_3 [kJ/kg]	262	262	261	260	259
h_4 [kJ/kg]	262	262	261	260	259
\dot{m} [kg/s]	0.0101	0.0107	0.0113	0.0119	0.0125
p_{cond} [bar]	14.3	14.1	13.7	13.3	12.8
p_{evap} [bar]	2.69	2.69	2.70	2.70	2.71
\dot{Q}_{HP} [W]	2154	2120	2075	2020	1955
\dot{Q}_{COOL} [W]	1362	1338	1306	1268	1223
\dot{W}_{comp} [W]	792	782	769	752	732
COP_{HP} [-]	2.72	2.71	2.70	2.69	2.67
COP_{COOL} [-]	1.72	1.71	1.70	1.69	1.67

Values for the pressure and enthalpies in table 5.2 can be used to plot the compressor cycle with twice the reference speed of the compressor and the baseline value for the chiller[W/K], which is show in the figure below.

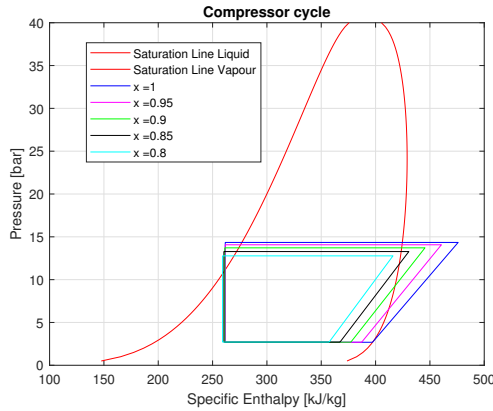


Figure 5.6: Figure showing the compressor cycle with twice the reference speed of the compressor and the baseline value for the chiller[W/K].

The figure of the compressor cycle changes in the same way as for the configuration in figure 5.3 when changing the vapour quality. The pressure decreases to a lower value in this case when the speed is set to twice the reference speed. When decreasing the quality the pressure decreases. When changing the speed the pressure decreases more to achieve the same quality.

The plot for \dot{Q}_{HP} with twice the reference speed of the compressor and the

baseline value for the chiller[W/K] is shown in the figure below.

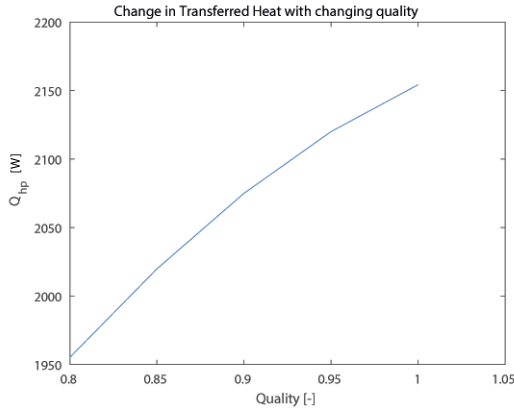


Figure 5.7: Figure showing how Q_{HP} changes for different vapour qualities x , with twice the reference speed of the compressor and the baseline value for the chiller[W/K].

Q_{HP} changes in the same way as for the configuration in figure 5.4, but Q_{HP} has a higher value with the increased speed. The figure below shows how COP_{HP} changes with twice the reference speed of the compressor and the baseline value for the chiller[W/K].

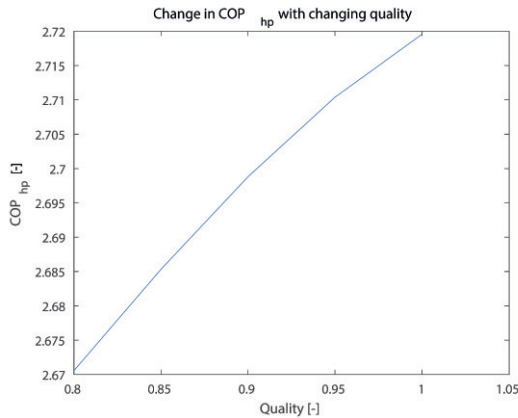


Figure 5.8: Figure showing COP_{HP} for different vapour qualities x , with twice the reference speed of the compressor and the baseline value for the chiller[W/K].

The value of COP_{HP} decreases when increasing the speed. This correlates with that both \dot{Q}_{HP} and \dot{W}_{comp} decreases with the speed but the output heat power decreases more.

The table below shows the results when running a simulation with reference speed of the compressor and twice the baseline value for the chiller[W/K].

Table 5.3: Table showing the simulation values for R134a with reference speed of the compressor and twice the baseline value for the chiller[W/K].

x	1	0.95	0.9	0.85	0.8
$A_{EXV} [mm^2]$	0.14	0.14	0.15	0.16	0.17
$h_1 [kJ/kg]$	398	388	378	368	358
$h_2 [kJ/kg]$	476	461	447	433	420
$h_3 [kJ/kg]$	249	251	252	252	253
$h_4 [kJ/kg]$	249	251	252	252	253
$\dot{m} [kg/s]$	0.0053	0.0056	0.0059	0.0062	0.0065
$p_{cond} [bar]$	15.0	14.8	14.6	14.4	14.1
$p_{evap} [bar]$	2.83	2.83	2.84	2.84	2.84
$Q_{HP} [W]$	1209	1186	1157	1123	1084
$Q_{COOL} [W]$	794	774	749	719	685
$\dot{W}_{comp} [W]$	415	412	408	404	399
$COP_{HP} [-]$	2.91	2.88	2.83	2.78	2.72
$COP_{COOL} [-]$	1.91	1.88	1.83	1.78	1.72

When using the values for the pressure and enthalpies in table 5.3 the following figure can be plotted:

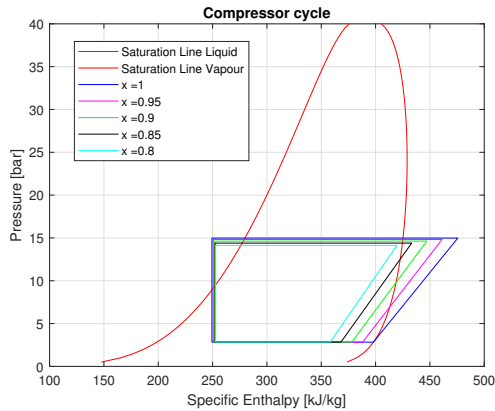


Figure 5.9: Figure showing the compressor cycle with reference speed of the compressor and twice the baseline value for the chiller[W/K].

When changing Ψ_{evap} the values of the pressure ratio, Q_{HP} and Q_{COOL} increases, but with a insignificant change. This can be seen when comparing table 5.1 and 5.3. In figure 5.9 the pressure on the high side does not decrease so much when comparing to figure 5.3.

Figure 5.9 shows the compressor cycle with reference speed of the compressor and twice the baseline value for the chiller[W/K].

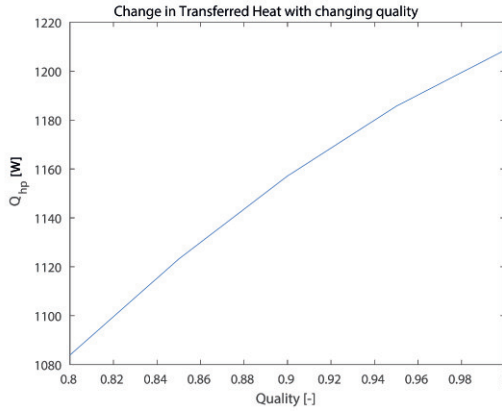


Figure 5.10: Figure showing how Q_{HP} changes for different vapour qualities x , with reference speed of the compressor and twice the baseline value for the chiller[W/K].

The value of Q_{HP} changes in the same way when changing the vapour quality. The figure below shows how COP_{HP} changes with the quality with reference speed of the compressor and twice the baseline value for the chiller[W/K].

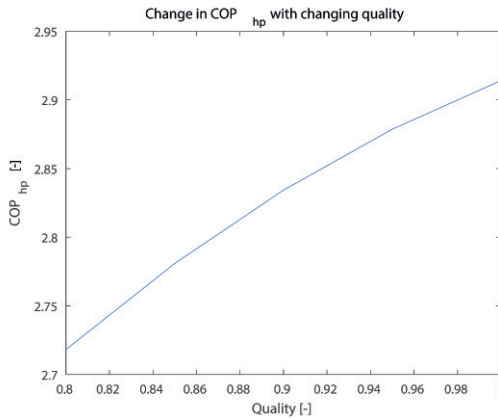


Figure 5.11: Figure showing COP_{HP} for different vapour qualities x , with reference speed of the compressor and twice the baseline value for the chiller[W/K].

COP_{HP} changes in the same way as earlier when changing the vapour quality. The table below shows the results when running a simulation with reference speed of the compressor and twice the baseline value for the chiller[W/K].

Table 5.4: Table showing the simulation values for R134a with reference speed of the compressor and twice the baseline value for the chiller[W/K].

x	1	0.95	0.9	0.85	0.8
A_{EXV} [m^2]	0.26	0.28	0.30	0.32	0.34
h_1 [kJ/kg]	398	388	378	368	358
h_2 [kJ/kg]	476	461	447	432	418
h_3 [kJ/kg]	264	264	263	263	262
h_4 [kJ/kg]	264	264	263	263	262
\dot{m} [kg/s]	0.0103	0.0109	0.0115	0.0121	0.0127
p_{cond} [bar]	14.8	14.6	14.3	13.9	13.5
p_{evap} [bar]	2.75	2.76	2.76	2.77	2.77
\dot{Q}_{HP} [W]	2203	2164	2115	2055	1986
\dot{Q}_{COOL} [W]	1387	1357	1319	1273	1220
\dot{W}_{comp} [W]	816	807	796	782	765
COP_{HP} [-]	2.70	2.68	2.66	2.63	2.60
COP_{COOL} [-]	1.70	1.68	1.66	1.63	1.60

The figure below shows the compressor cycle with twice the reference speed of the compressor and twice the baseline value for the chiller[W/K].

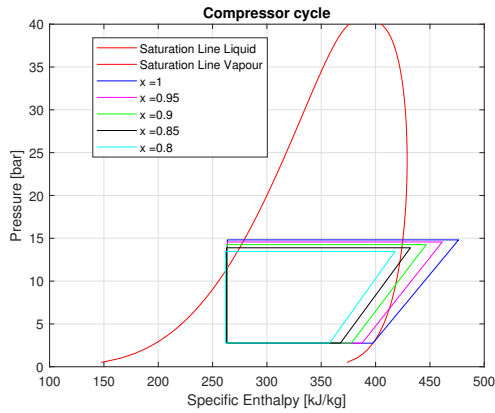


Figure 5.12: Figure showing the compressor cycle with twice the reference speed of the compressor and twice the baseline value for the chiller[W/K].

When increasing both the speed with the same value of Ψ_{evap} the changes are similar as when changing the speed for Ψ set twice the baseline value. The pressure ratio, Q_{HP} , Q_{COOL} increases during these changes, but COP_{HP} decreases. The next figure below shows how Q_{HP} changes with the quality.

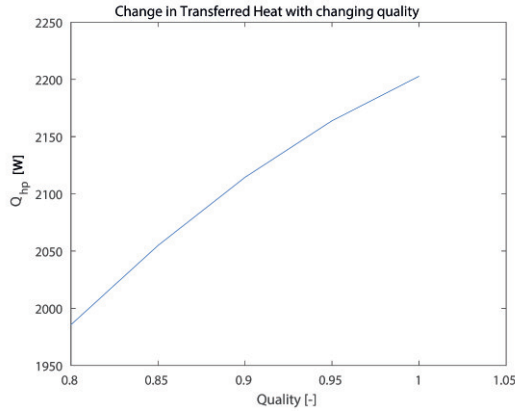


Figure 5.13: Figure showing how Q_{HP} changes for different vapour qualities x , with twice the reference speed of the compressor and twice the baseline value for the chiller[W/K].

The value of Q_{HP} changes in the same way as before when changing the quality. The figure below shows how COP_{HP} changes with the quality.

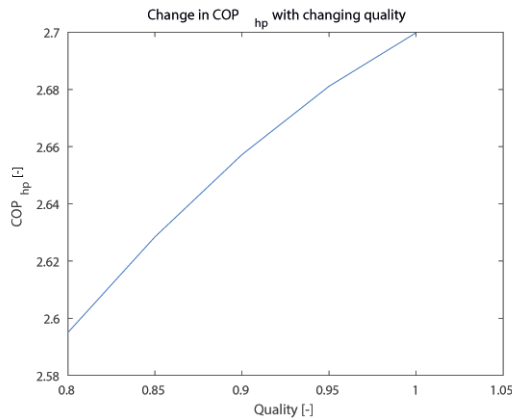


Figure 5.14: Figure showing COP_{HP} for different vapour qualities x , with twice the reference speed of the compressor and twice the baseline value for the chiller[W/K].

As expected COP_{HP} also changes in the same way as earlier when changing the vapour quality. The table below show the results when simulating with 4 times the reference speed of the compressor and twice the baseline value for the chiller[W/K].

Table 5.5: Table showing the simulation values for R134a with 4 times the reference speed of the compressor and twice the baseline value for the chiller[W/K].

x	1.00	0.95	0.90	0.85	0.80
$A_{EXV} [mm^2]$	0.51	0.55	0.59	0.64	0.69
$h_1 [kJ/kg]$	397	387	377	367	357
$h_2 [kJ/kg]$	477	461	445	430	415
$h_3 [kJ/kg]$	268	267	266	264	262
$h_4 [kJ/kg]$	268	267	266	264	262
$\dot{m} [kg/s]$	0.0194	0.0206	0.0218	0.0230	0.0242
$p_{cond} [bar]$	14.1	13.7	13.3	12.8	12.2
$p_{evap} [bar]$	2.61	2.61	2.62	2.63	2.64
$\dot{Q}_{HP} [W]$	4041	3986	3910	3815	3703
$\dot{Q}_{COOL} [W]$	2494	2461	2416	2361	2295
$\dot{W}_{comp} [W]$	1547	1525	1494	1455	1408
$COP_{HP} [-]$	2.61	2.61	2.62	2.62	2.63
$COP_{COOL} [-]$	1.61	1.61	1.62	1.62	1.63

The results when simulating with a higher speed implies to a higher heating power \dot{Q}_{HP} . The heating power still decreases when changing the vapour quality and keeping the speed at a constant value.

5.2.2 R1234yf

This section treats the results for R1234yf as working medium in the simulation. The table below shows the results when running the simulation with 4 times the reference speed of the compressor and twice the baseline value for the chiller[W/K].

Table 5.6: Table showing the simulation values for R1234yf with 4 times the reference speed of the compressor and twice the baseline value for the chiller[W/K].

x	1.00	0.95	0.90	0.85	0.80
A_{EXV} [mm ²]	0.42	0.45	0.48	0.52	0.56
h_1 [kJ/kg]	383	373	364	355	346
h_2 [kJ/kg]	469	453	439	424	410
h_3 [kJ/kg]	277	276	275	274	273
h_4 [kJ/kg]	277	276	275	274	273
\dot{m} [kg/s]	0.016	0.017	0.018	0.019	0.020
p_{cond} [bar]	13.6	13.3	13.0	12.6	12.1
p_{evap} [bar]	2.00	2.00	2.01	2.01	2.02
\dot{Q}_{HP} [W]	3078	3017	2942	2853	2751
\dot{Q}_{COOL} [W]	1700	1657	1603	1540	1468
\dot{W}_{comp} [W]	1378	1361	1339	1314	1283
COP_{HP} [-]	2.23	2.22	2.20	2.17	2.14
COP_{COOL} [-]	1.23	1.22	1.20	1.17	1.14

The figure below shows how the compressor cycle changes when the quality is changed.

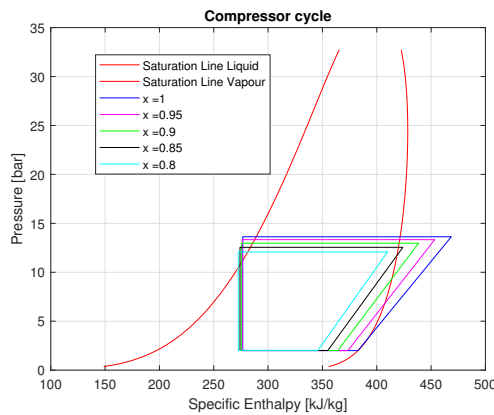
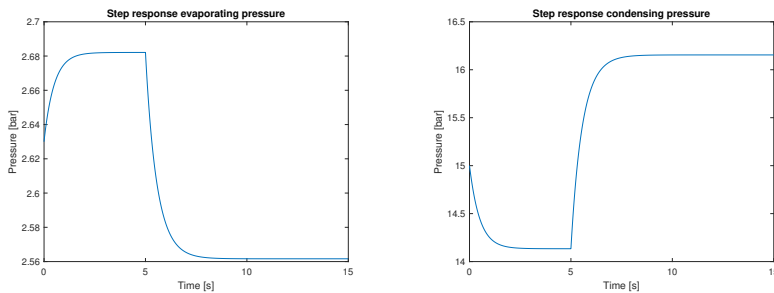


Figure 5.15: Figure showing the compressor cycle for R1234yf when running the simulation with 4 times the reference speed of the compressor and twice the baseline value for the chiller[W/K].

Figure 5.15 shows that the compressor cycle changes in the same way as for R134a. The heating power decreases also in this case when changing the vapour quality.

5.2.3 Step results

To evaluate the dynamics of the model a step was taken in compressor speed (2.1 to 2.2 times the reference speed) while the area of the expansion valve remained unchanged. Figure 5.16 shows the step response of the evaporating pressure as well as the condensing pressure.



(a) Step response of the evaporating pressure. (b) Step response of the condensing pressure.

Figure 5.16: Step response of evaporating and condensing pressure.

5.3 Validation results

The following section treats the validation of the components in the heat pump. The compressor and chiller is compared and validated with measured values from rig tests and car tests. The condenser is assumed to have complete condensation and the expansion valve is a static component with a well known equation for the pressure drop. The values in the following plots are not display with respect to censured data. Validation was only performed with data with superheated gas into the compressor, i.e. no liquid content.

Compressor

The following figures shows how well the model for the mass flow, discharge temperature and power matches the measured values.

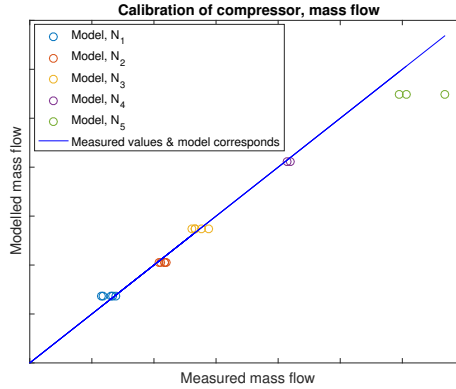


Figure 5.17: Figure showing how the modelled and measured mass flows corresponds. The x- and y-axis has the same values(scale 1:1) and N_1 , N_2 , N_3 , N_4 and N_5 are different test speeds.

The mass flow in the figure above shows a good match, but have some model faults for higher mass flows. The polytropic efficiency η_{pol} is changed to achieve a satisfactory match between the data and the model. The volumetric efficiency is set to a constant value in the model and this explains why the values for a selected speed differ from the line.

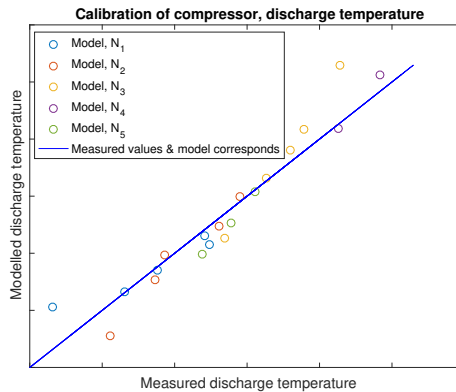


Figure 5.18: Figure showing how the modelled and measured temperature corresponds. The x- and y-axis has the same values(scale 1:1) and N_1 , N_2 , N_3 , N_4 , N_5 are different test speeds.

The figure above shows how the modelled discharge temperature differ from the measured. The discharge temperature is modelled with the assumption of polytropic process where there is no heat exchange with the surroundings.

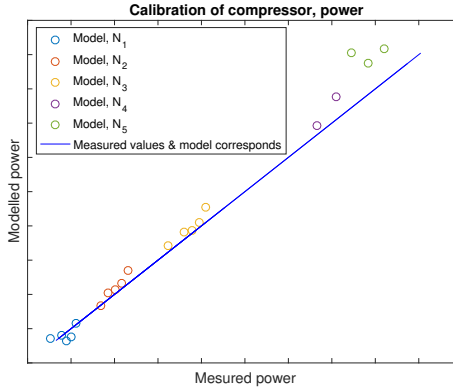


Figure 5.19: Figure showing how the modelled and measured power corresponds. The x- and y-axis has the same values (scale 1:1) and N_1 , N_2 , N_3 , N_4 and N_5 are different test speeds.

Figure 5.19 shows how the modelled power corresponds with the measured. The modelled power differ when the power has a higher value.

Chiller

For the chiller a Ψ_{evap} [W/K] is calculated for the measured values. This Ψ_{evap} is then used in the model to see how well the modelled temperature out of the chiller matches with the measured. The following plot shows how much the model differ from the measured values with data with superheated gas into the compressor.

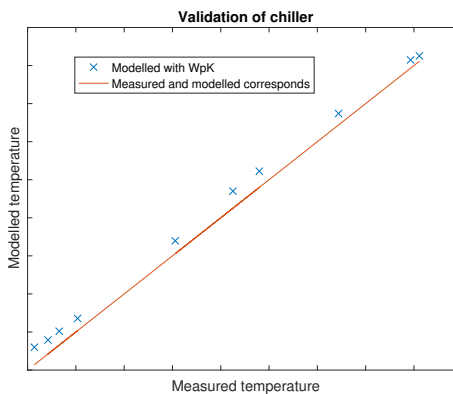


Figure 5.20: Figure showing how the model and measured temperature in the chiller corresponds.

The adapting between measured and modelled values is made to be as accurate as possible to the output temperature but another error source is the vapour quality x . The vapour quality also needs to be matched in a satisfactory way.

Condenser and Expansion valve

The condensation in the condenser is assumed to be complete (chapter 4) and is delimited with non existing measured data. The outline regarding the goal of 10 kW in heating power relates to how much thermal power possible to obtain from the condenser refrigerant. Since the condensation is complete and delimited data, the validation is not necessary for the condenser.

The expansion valve is treated as a static component with fast dynamics. The validation of the expansion valve is delimited with non existing measured data and the modelling is done with a well known component equation. The validation is therefore not necessary for the expansion valve.

Complete heat pump model

The whole simulation model is validated against a cycling AC-test with large transients to check if the model acts in the right way. The pressures are deemed to be most important to validate due to condensing and evaporating temperatures following the behaviour of the pressure. The behavior was considered adequate for the calculation model.

When comparing test results with the simulation step results in figure 5.16, the simulated pressure on the high and low side corresponds with the measured results with a reasonable time constant. This shows that the simulation model acts in the same way as the measured results.

6

Discussion

In this chapter a discussion is made regarding the modelling approach, all the assumptions made in the thesis, the delimitations and the results.

6.1 Method

During the modelling process a several assumptions were made to simplify the modelling process. The components of the heat pump have each separately a couple of assumptions that relates to the related research regarding heat pumps, which is described in chapter 5.

The compressor was assumed to be isentropic which leads to that the modelling does not take the heat transfer between the compressor and the surroundings into account. Also the process is reversible which does not correspond to the real process. The polytropic efficiency is calibrated against test data but the volumetric efficiency is set to a constant value. This is a simplification to avoid a specific model for the volumetric efficiency. How the constant value of the volumetric efficiency effects the mass flow is shown in the figure 5.17.

The heat exchanger was assumed to be circular pipes with a uniform area that has thin walls. This simplifies the modelling but also gives a less accurate result. When not modelling the conduction between the wall and the fluids/gases the heat transfer between the mediums is not completely modelled. For a general case this type of modelling is preferable but less accurate for a more specific case where more information regarding the heat exchanger is provided. Also the construction of the heat exchanger is a general construction with a counter flow configuration which does not correspond to all types of heat exchangers. The pressure drop over the heat exchanger is assumed to be small which is an assumption that effects the outcome of the results.

One of the most essential assumptions regarding the two phase zone is that a

mean void quality is used to calculate the mean density in the control volume. The heat exchanger is therefore treated as a mean value model where the density in each phase zone (vapour, mixture and liquid) can be treated as a mean value. In order to make this modelling approach more accurate each zone of the condenser can be divided into more finite parts and the mean density can be calculated in each part.

The evaporator has only one zone in the model when the request was to investigate the out coming results when changing the vapour quality. There is no model for the overheated zone of the evaporator, which makes the results less accurate if the purpose is simulation with overheating in the evaporator. When modelling the chiller the general parameter Ψ_{evap} is set to a constant value which is a rough assumption regarding the chiller. Ψ_{evap} is a value to describe how much heat capacity per temperature difference between the refrigerant and water/glycol that can be transferred to the heat pump. This assumption is tested in the validation part(5.3) where the temperature out of the chiller differs little from the actual tests made in cars and in rigg test.

The condenser is assumed to have complete condensation, which means that a certain subcooling is obtained in all simulations. This is an assumption made in relation to the purpose of the thesis, which is investigating how the quality effects the mass flow and how this effects the output heating power. The condensation can be complete by using filters and turbulators, and the out come of this project is more to investigate the quality in the evaporator.

The whole model has an ideal modelling approach. The COP and \dot{Q}_{HP} values is for the ideal case and to get a more accurate result there is a need of modelling of more components. The power in the compressor is the thermodynamic power and by modelling the electric motor that controls the compressor, modelling of the fan in the radiator and modelling of pumps in the water and water/glycol circuits will contribute to a better result. Also the efficiencies of the components needs to be modelled.

The modelling is done in a mathematical way based on psychical laws and the delimitation with a more theoretical investigation compared to a more empirical study leads to some deviations compared to the real case. On the other hand the simulation model is created with the ability to simulate general cases and investigate different condition for the heat pump system.

6.2 Results

The different vapour qualities are achieved by changing the area of the expansion valve. Therefore the pressure drop in the heat pump system decreases slightly even though the mass flow rate is increasing. Since the heat transfer rate \dot{Q}_{HP} is a product of the mass flow rate and the enthalpy loss over the condenser the objective for this thesis was to increase the heat capacity by increasing the density of the refrigerant and thereby increasing the mass flow. It is clear by the results that a decrease in vapour quality increases the total mass flow rate but the heat transfer is decreasing. This can be explained by the decrease of specific enthalpy

of the refrigerant at the outlet of the evaporator. This difference in enthalpy between the different vapour qualities is then increased by the isentropic compressor. This means that when the vapour quality is decreased slightly, which leads to the specific cooling ($h_1 - h_4$) decreasing slightly, the specific heating ($h_2 - h_3$) is decreased even more. This loss in specific heating is larger than the increase one gets in mass flow rate. It is also interesting to see that even the coefficient of performance is decreasing even though the compressor work is decreasing meaning that the output heat \dot{Q}_{HP} is decreasing faster than the power consumption of the compressor.

When comparing the two refrigerants R134a and R1234yf one can see that both \dot{Q}_{HP} and \dot{Q}_{cool} is overall lower for R1234yf. This result is not very unexpected since the specific enthalpies for saturation are closer together, which can be seen in figure 5.1. Since they are closer together it means that it requires less energy to "transform" the refrigerant from one phase to another, this all results in less output/input heat transferred.

To reach the goal of transferring 10kW from the refrigerant to the water, at the condenser, a larger compressor is probably needed since \dot{Q}_{HP} did not increase by decreasing the vapour quality. At least if the only source of heat is the ambient temperature. If heat can be taken from other sources (like mentioned above) such as other electrical components or even waste heat from a conventional engine in the case of a hybrid vehicle the goal can probably be met but a larger compressor is still most likely to be needed.

7

Conclusions

7.1 Conclusions

The thesis work has resulted in an investigation regarding the vapour quality in a heat pump simulation when having a surrounding temperature of 0° C. The results for R134a shows that when changing the vapour quality the mass flow increases as expected since the density increases. The heating capacity (Q_{HP}) is on the other hand decreasing with the change of vapour quality. This depends on that the increase in mass flow does not increase enough compared to to decrease in specific heating.

Changing the volume and the speed of the compressor results in a larger mass flow rate without a significant decrease in specific heating which makes it possible to achieve the goal of 10 kW heating power. This change of compressor volume leads to a different size on the compressor which requires more space than the original AC compressor. When running the simulation with R1234yf instead of R134a similar results are obtained. The difference in properties for the different refrigerants results in a lower heating capacity for R1234yf. On the other hand R1234yf has a lower impact on the environment and is a refrigerant for the future.

7.2 Further work

The increasing interest in hybridization and electrification makes the topic regarding heat pumps in vehicles very important. The use of waste heat and surrounding air to heat/cool the cabin and components is a future development. It is worth noting that these results are for the delimitations and assumptions made in this thesis and the simulation model can be further developed. The compressor can be modelled with an electric motor where the input power controls the com-

pressor. The condenser is assumed to have complete condensation, and instead of this assumption the complete condensation process can be modelled with filters and other components. The evaporator is simplified with Ψ_{evap} [W/K] which is a general description of a heat exchanger's capacity. This simplification can be developed by expanding the modelling approach from a simple model to a more detailed chiller model.

One interesting thing to study in the future is the impact of a less ideal compressor model. For instance the inside walls of the compressor are rather warm and therefore there may be an additional heat exchange and with evaporation of droplets on hot surfaces. Meaning that the enthalpy at the output of the compressor in fact is not decreasing as much as in these results. Therefore a less ideal compressor model might be interesting to study.

The whole simulink model can be expanded with other components that require heating/cooling or be integrated into an existing vehicle model. This will result in a model that better describes the ability of heating the cabin/components in cold environments. The vehicle model integrated with the heat pump model can be used to simulate drive cycles and analyze the heating/cooling performance in hybrid and electric vehicles. A controller that takes temperature changes inside the vehicle into consideration is also a thing that could be added. For example a bus that opens its doors at a bus stop on a cold winter day and thereby decreasing the overall temperature inside the cabin.

Appendix

A

Appendix A

A.1 Map function plots

The figure A.1 shows the specific heat capacity, c_p , for saturated vapour and liquid for different pressures.

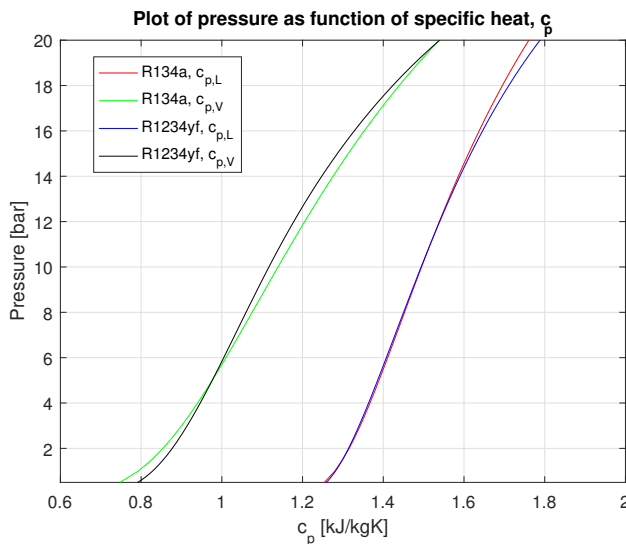


Figure A.1: Figure showing the specific heat capacity c_p for the refrigerants.

The figure A.2 shows the specific heat capacity, c_v , for saturated vapour and liquid for different pressures.

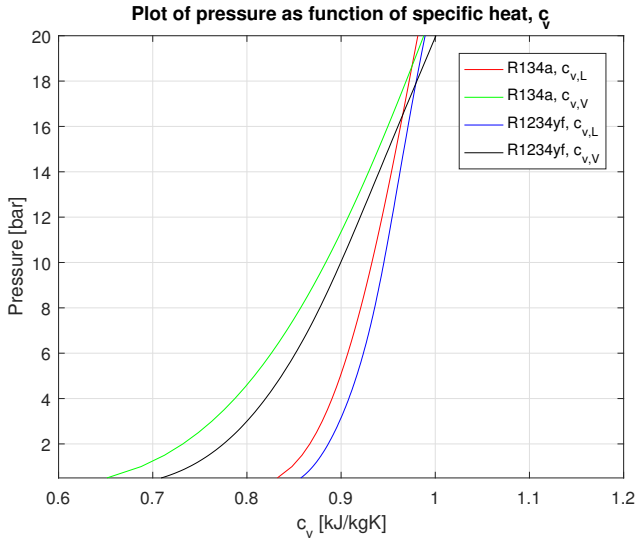


Figure A.2: Figure showing the specific heat capacity c_v for the refrigerants.

The figure A.3 shows the conductivity for saturated vapour and liquid changes for different pressures.

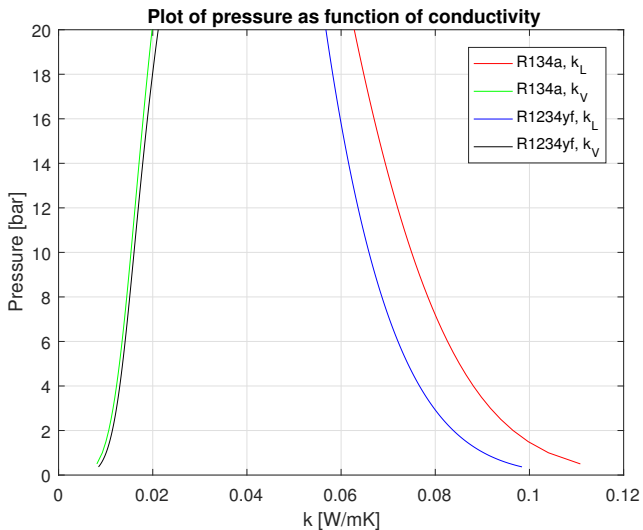


Figure A.3: Figure showing the conductivity for the refrigerants.

The figure below shows how the boiling temperature for the two refrigerants changes with the pressure.

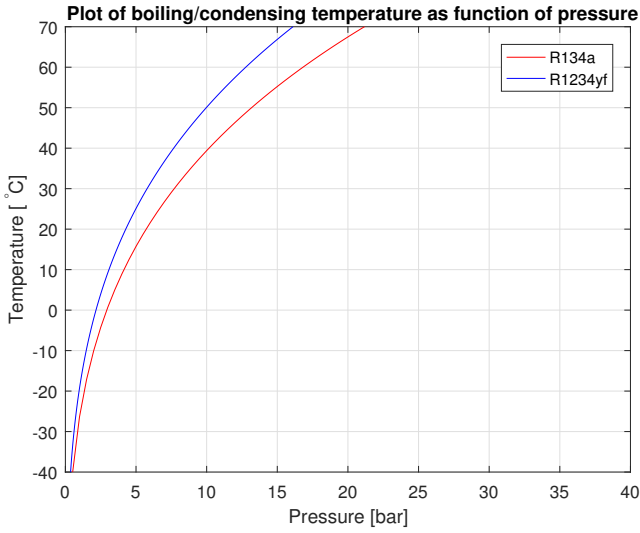


Figure A.4: Figure showing the boiling temperature for the refrigerants.

The figure A.5 shows how the freezing temperature changes with the volume percentage glycol.

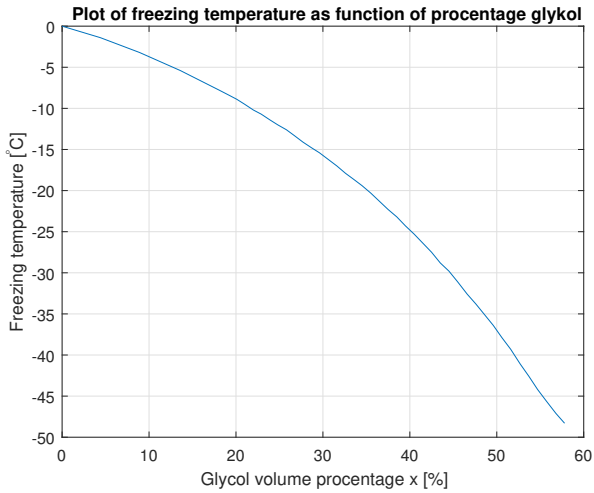


Figure A.5: Figure showing the freezing point for the water/glycol mixture for different volume percentage of glycol.

Bibliography

- [1] The Linde Group 2018. Solstice 1234yf (r1234yf). Website, 2018. URL http://www.linde-gas.com/en/products_and_supply/refrigerants/hfo_refrigerants/solstice_yf/index.html. Online; 2018-04-19. Cited on page 20.
- [2] The Linde Group 2018. R134a. Website, 2018. URL http://www.linde-gas.com/en/products_and_supply/refrigerants/hfc_refrigerants/r134a/index.html. Online; 2018-01-26. Cited on page 20.
- [3] The Linde Group 2018. R744 (carbon dioxide). Website, 2018. URL http://www.linde-gas.com/en/products_and_supply/refrigerants/natural_refrigerants/r744_carbon_dioxide/index.html. Online; 2018-01-26. Cited on page 20.
- [4] AirconCars. How air conditioning works. Website, 2018. URL http://www.airconcars.com/html/how_it_works.html. Online; 2018-01-26. Cited on page 19.
- [5] Sorour Alotaibi, Mihir Sen, Bill Goodwine, and K.T. Yang. Controllability of cross-flow heat exchangers. *International Journal of Heat and Mass Transfer*, 47, 2004. Cited on page 27.
- [6] Magnus Andersson and Henrik Jerregård. Modelling and control of vapour compression refrigeration systems. Technical report, Automatic Control at Linköping Institute of Technology, 3 1999. Cited on pages 13 and 36.
- [7] Stefano Badiali and Stefano Colombo. Dynamic modelling of mechanical heat pumps for comfort heating. Technical report, Royal Institute of Technology, Politecnico di Milano, 03 2009-2010. Cited on pages 26, 30, 38, and 43.
- [8] Robert T Balmer. *Modern Engineering Thermodynamics*. Elsevier Inc, 2011. Cited on pages 5, 6, and 20.

- [9] Michael Baster Eric. Modelling the performance of air source heat pump systems. Technical report, University of Strathclyde engineering, 12 2011. Cited on page 26.
- [10] The Dow Chemical Company. Engineering and operating guide. pdf, 2008. URL http://msdssearch.dow.com/PublishedLiteratureDOWCOM/dh_010e/0901b8038010e413.pdf?filepath=/heattrans/pdfs/noreg/180-01190.pdf&fromPage=GetDoc. Online; 2018-05-20. Cited on page 33.
- [11] Manuel R. Conde. A contribution to heat pump design by simulation. *Juris Druck, Verlag Dietikon, SWISS FEDERAL INSTITUTE OF TECHNOLOGY ZURICH*, (1970):71–123, 1992. Cited on pages 12 and 19.
- [12] P. Domanski and D. Didion. Computer modeling of the vapor compression cycle with constant flow area expansion device. Technical report, National Bureau of Standards Building Science Series 155, 5 1983. Cited on pages 27 and 28.
- [13] Ronald E. Domitrovic, Vince C. Mei, and F.C. Chen. Simulation of an automotive heat pump. *Materials Science & Engineering Database*, 103:291–296, 1997. Cited on page 25.
- [14] Ingvar Ekroth and Eric Granryd. *Tillämpad termodynamik*. Studentlitteratur, 1 edition, 2006. Cited on page 7.
- [15] EmersonClimate. Co2 as a refrigerant-series introduction. Website, 2015. URL <https://emersonclimateconversations.com/2015/04/16/co2-as-a-refrigerant-series-introduction/>. Online; 2018-01-26. Cited on page 20.
- [16] P Erhard, D Etling, U Muller, U Riedler, K.R Sreenivasan, and J Warnatz. *Prandtl - Essentials of fluid mechanics*. Springer, third edition edition, 2010. Cited on page 30.
- [17] S.K. Fisher and C.K. Rice. The oak ridge heat pump models: 1. a steady-state computer design model for air-to-air heat pumps. Technical report, Oak Ridge National Laboratory, 8 1983. Cited on page 28.
- [18] J. M. Gordon and Kim Choon Ng. Thermodynamic modeling of reciprocating chillers. *Journal of Applied Physics*, 1994. Cited on page 28.
- [19] Arkadiusz Guźda and Norbert Szmolke. Compressors in heat pumps. *Machine Dynamics Research*, 39(2):71–83, 2015. Cited on page 10.
- [20] Industrial heat pumps. Refrigerants. Website, 2018. URL http://industrialheatpumps.nl/en/how_it_works/refrigerants/. Online; 2018-01-26. Cited on page 19.

- [21] Honeywell. Honeywell refrigerants. Website, 2018. URL <https://fluorineproducts-honeywell.com/refrigerants/>. Online; 2018-02-20. Cited on page 33.
- [22] M. Hosoz and M. Direk. Performance evaluation of an integrated automotive air conditioning and heat pump system. *Energy Conversion and Management*, 47:545–559, 2005. Cited on page 23.
- [23] M. Hosoz, M. Direk, K.S. Yigit, M. Canakci, A. Turkcan, E. Alptekin, A. Sanli, and A.F. Ozguc. Experimental performance of an r134a automobile heat pump system coupled to the passenger compartment. *World Renewable Energy Congress 2011*, page 3605–3612, 2011. Cited on page 24.
- [24] Cheng-Ting Hsu, Da-Jeng Yao, Ke-Jyun Ye, and Ben Yu. Renewable energy of waste heat recovery system for automobiles. *Journal of Renewable and sustainable energy 2*, (81):155–159, 2010. Cited on page 25.
- [25] Md Islam Mafizul and Md Salam Abdul. Modelling and control system design to control water temperature in heat pump. Technical report, Karlstad Universitet, 12 2013. Cited on page 25.
- [26] Amir Jokar, Mohammad H. Hosni, and Steven J. Eckels. A heat pump for automotive applications. pages 1–13, 2005. Cited on page 23.
- [27] Yasuo Katayama, Nobuya Nakagawa, Tomoki Hase, Manabu Suzuki, and Yasunobu Joubouji. Development of heat pump system for plug-in hybrid vehicles. *Mitsubishi Heavy Industries Technical Review*, 54(2):54–56, 2017. Cited on page 24.
- [28] Ramesh K.Shah and Dusan P.Sekulic'. *Fundamentals of heat exchanger design*. John Wiley Sons, INC., 2003. Cited on pages 10, 11, and 12.
- [29] Lennart Ljung and Torkel Glad. *Modeling and Identification of Dynamic System*. Studentlitteratur AB, 1 edition, 2016. Cited on page 21.
- [30] J. W. MacArthur. Transient heat pump behaviour: a theoretical investigation. *Butterworth Et Co*, 7(2):123–132, 1984. Cited on page 26.
- [31] National Institute of Standards and Technology. Thermophysical properties of fluid systems. Website, 2017. URL <https://webbook.nist.gov/chemistry/fluid/>. Online; 2018-04-13. Cited on page 33.
- [32] Frank P.Incropera, David P.Dewitt, Theodore L.Bergman, and Adrienne S.Lavine. *Fundamental of Heat and Mass Transfer*. John Wiley Sons, INC., sixth edition, 2007. Cited on page 16.
- [33] Ioan Sarbu and Sebarchievici Calin. *Ground-Source Heat Pumps*. Elsevier Ltd, 2016. Cited on pages 8, 9, and 10.
- [34] Róbert Sánta. The analysis of two-phase condensation heat transfer models based on the comparison of the boundary condition. *Acta Polytechnica Hungarica*, 9(6):167–180, 2012. Cited on page 30.

-
- [35] Seiichi Yamaguchi, Daisuke Kato, Kiyoshi Saito, and Sunao Kawai. Development and validation of ststic simulation model for CO_2 heat pump. *International Journal of Heat and Mass Transfer*, 54, 2011. Cited on page 27.
- [36] J. Yang. Potential applications of thermoelectric waste heat recovery in the automotive industry. pages 155–159, 2005. Cited on page 25.
- [37] Chuang Yu and K.T. Chau. Thermoelectric automotive waste heat energy recovery using maximum power point tracking. *Elsevier Ltd*, page 1506–1512, 2009. Cited on page 25.